The Informational Value of Pressure-Based Proxies for Past Storm Activity

(Vom Fachbereich Geowissenschaften der Universität Hamburg im Jahr 2013 als Dissertation angenommene Arbeit)

O. Krüger

wissen
schafft
nutzen

Helmholtz-Zentrum
Geesthacht
Zentrum für Material- und Küstenforschung

The Informational Value of Pressure-Based Proxies for Past Storm Activity

O. Krüger

The Informational Value of Pressure-Based Proxies for Past Storm Activity

(Vom Fachbereich Geowissenschaften der Universität Hamburg im Jahr 2013 als Dissertation angenommene Arbeit)

Oliver Krüger

60 Seiten mit 12 Abbildungen und 4 Tabellen

Abstract

Air pressure readings and their variations are commonly used to make inferences about storm activity. More precisely, it is assumed that the variation of annual and seasonal statistics of several pressure-based proxies describes changes in the past storm climate qualitatively – an assumption that has yet to be proven.

This work presents a systematic evaluation of several cases of such pressure-based proxies for storm activity. The results indicate that the statistics of geostrophic wind speeds are a valuable proxy for describing past storm activity. On the contrary, results from analyses of proxies derived from pressure readings from single stations show that the informational value of the statistics of such proxies is lower.

Pressure proxies also make it possible to determine how realistically historic climate simulations or reanalyses reproduce the past storm climate and associated long-term trends. The present work compares the storm climate over the Northeast Atlantic from the Twentieth Century Reanalysis (20CR) dataset with storminess derived from pressure observations reaching back to the 1880s through using geostrophic wind speed statistics. The results point to large inconsistencies between storminess in 20CR and storminess derived from observations in the 19th and mid-20th century in that region due to an increasing number of assimilated pressure observations over time.

Der Informationsgehalt luftdruckbasierter Proxies für vergangene Sturmaktivität

Zusammenfassung

Aus Luftdruckmessungen und Luftdruckschwankungen abgeleitete Statistiken werden im Allgemeinen dazu benutzt Rückschlüsse auf das vergangene Sturmklima zu ziehen. Genauer gesagt wird angenommen, dass Veränderungen von saisonalen und jährlichen Statistiken von luftdruckbasierten Proxys die Veränderungen des vergangenen Sturmklimas qualitativ beschreiben. Diese Annahme ist bisher unbewiesen.

In dieser Arbeit werden mehrere luftdruckbasierte Proxys für Sturmaktivität systematisch evaluiert. Es zeigt sich, dass geostrophische Windstatistiken ein nützlicher Proxy sind um historische Sturmaktivität zu beschreiben. Resultate aus der Evaluierung von Proxys, die auf Luftdruckbeobachtungen von einzelnen Stationen beruhen, belegen, dass diese im Gegenzug einen verringerten Informationsgehalt besitzen.

Luftdruckbasierte Proxys ermöglichen es ebenfalls zu beurteilen, zu welchem Grad historische Klimasimulationen, bzw. Reanalysen, es ermöglichen, das vergangene Sturmklima und dazugehörige Langzeittrends realistisch zu beschreiben. Die vorliegende Arbeit vergleicht dazu das Sturmklima seit den 1880ern über dem Nordostatlantik im „Twentieth Century Reanalysis"(20CR) Datensatz mit dem Sturmklima, das aus Luftdruckbeobachtungen abgeleitet wird. In beiden Fällen werden geostrophische Windgeschwindigkeitsstatistiken benutzt um Aussagen zu treffen. Die Ergebnisse weisen auf große Inkonsistenzen zwischen dem aus Beobachtungen abgeleiteten Sturmklima und dem in der 20CR-Reanalyse hin. Dabei werden die größten Diskrepanzen im Zeitraum zwischen dem Ende des 19. bis hin zur ersten Hälfte des 20. Jahrhunderts gefunden. Die Ergebnisse lassen sich durch eine zeitlich zunehmende Anzahl von in die Reanalyse assimilierten Beobachtungen erklären.

Contents

1   Introduction

Changes in storminess affect ecosystems and living conditions. The evaluation of the past storm climate imparts valuable knowledge for people and countries, also in connection with anthropogenic climate change. For instance, the strong increase in storminess over North Europe from the 1960s to the 1990s raised concerns about the impact of possible anthropogenic influences on wind speeds and wave heights (Schmidt and von Storch, 1993). Several studies of climate change, in which possible future scenarios of increased anthropogenic forcing were considered, suggest shifting storm tracks that would lead to regional changes in mean and extreme wind speeds (Pinto et al., 2010; Pryor et al., 2012). The assessment of the past storm climate helps to understand whether trends and changes of storminess exceed the natural variability of storminess, which would support the argument of a changing storm climate along with anthropogenic climate change.

Nonetheless, deriving information about the past storm climate is still a rather difficult subject in modern atmospheric and climate sciences. The discussion about past storminess is usually hampered by the lack of long and homogeneous time series of wind speed observations. Inhomogeneities are caused by observational routines and analyses, type and accuracy of used instruments, as well as the station surroundings and relocations (Trenberth et al., 2007).

There are some well documented examples for such inhomogeneities in wind speed recordings, for instance, the monthly mean wind speed time series of McInnes Island (located north of Vancouver Island, BC, Canada). It shows three sudden in- or decreases caused by a change of instruments in 1963 and station relocations in 1973 and 1982 (Wan et al., 2010). Another example deals with the yearly mean wind speed time series in the German Bight (see Figure 1.1), where the Helgoland time series shows a sudden increase by 1.25 m/s in 1989 (Lindenberg, 2011) due to two station relocations in one year. It should be noted that also improvements in the observational framework can lead to inhomogeneities (Shepherd and Knutson, 2007), which is nicely illustrated in Weisse and von Storch (2009) and shown in Figure 1.2. Both the organisation of international weather services and the onset of satellite measurements becoming available have introduced inhomogeneities related to information exchange and improved supervision.
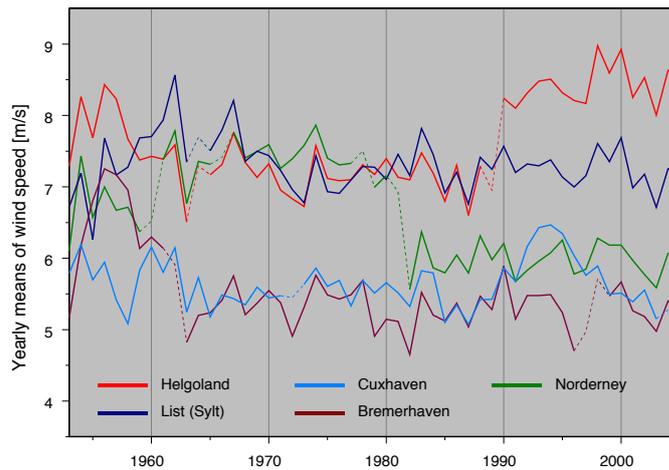
FIGURE 1.1: Yearly mean wind speed time series in the German Bight (from Lindenberg, 2011).
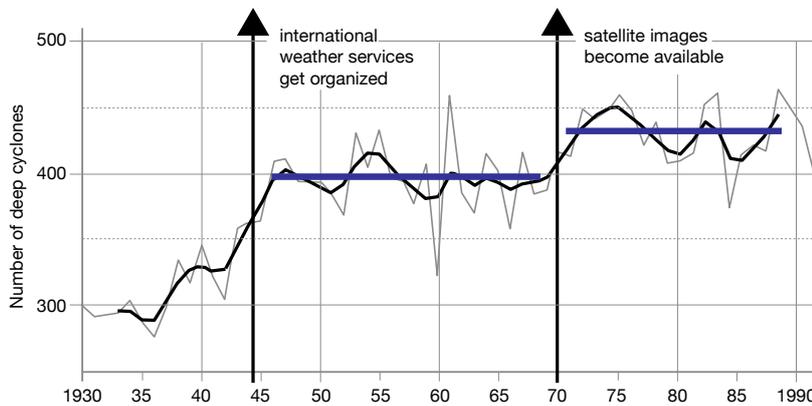
FIGURE 1.2: Number of deep cyclones detected in daily German weather maps of the North Atlantic (after Weisse and von Storch, 2009).

One approach feasible for the mid-latitudes to counteract such problems is to derive substitute or proxy time series from a meteorological variable that does not suffer from inhomogeneities and has been observed for a sufficiently long time. The air pressure is such a variable, with records of observations reaching back to the 1750s in some cases (e.g. Matulla et al., 2011).

Air pressure-based proxies have been used for some decades to determine past storminess from pressure observations. Two different classes of proxies exist, one that builds upon pressure observations from a single station, and one that requires pressure readings from multiple stations. Both classes share the common assumption that the variation of their statistics describes the variation of the statistics of surface wind speeds qualitatively. This assumption had not been proven before parts of this work were published. One main aim of this doctoral thesis is to close this gap by a systematic evaluation of the informational

content of pressure-based proxies for storm activity. In this work, the correlation between statistics of ground level wind speeds and pressure-based proxies is used as a measure for the informational content of such proxies.

Because such an analysis needs long and homogeneous wind time series (which are hardly ever available from observations), diagnostic 10-m wind and surface air pressure fields from the spectrally nudged and NCEP/NCAR-driven (Kistler et al., 2001) regional model REMO (see Feser et al., 2001; Weisse et al., 2009) over the period 1959-2005 are employed here. These fields are part of the coastDat-dataset[1]. In a $0.5° \times 0.5°$ spatial (around 50 - 60 km) and 1-hourly temporal resolution, the used fields cover Europe and the North Atlantic. Several studies (e.g. Weisse et al., 2005; Koch and Feser, 2006; Kunz et al., 2010) show that REMO adequately simulates wind speeds over land and sea. More importantly, within REMO the data are dynamically consistent. For that reason, the aforementioned simulated fields are used for the assessment.

In the following chapter, the individual air-pressure based proxies for past storminess are introduced. Sections 2.1 and 2.2 cover the proxies based on pressure readings from single and multiple stations. These sections summarize the evaluation of the informational value of each individual proxy. In Chapter 3, the storm climate in the Twentieth Century Reanalysis (20CR) dataset is assessed using a multiple-station based proxy (i.e. geostrophic wind speed statistics) derived from observations and the reanalysis. Afterwards, in Chapter 4, further possible research dealing with pressure proxies is presented, followed by a general conclusion (Chapter 5).

---

[1]available at `http://www.coastdat.de`

2 Pressure-Based Proxies for Storm Activity

2.1 Proxies Based on Pressure Readings from Single Stations

In general, the proxies based on air pressure readings from a single station originate from synoptic experience. They are expected to reflect cyclone activity and storminess changes in the area around a weather station. Five different proxies are commonly used throughout the literature. Namely, they are the *number of deep lows* (that is the number of local pressure observations below a chosen threshold), *lower percentiles of pressure*, *the frequency of absolute pressure tendencies exceeding certain thresholds*, as well as *high percentiles* and *mean values of absolute pressure tendencies*. The proxies have been used in several studies analyzing storminess in the North Atlantic and European regions (e.g. Schmith et al., 1998; Jonsson and Hanna, 2007; Allan et al., 2009; Bärring and von Storch, 2004; Bärring and Fortuniak, 2009; Alexander et al., 2005; Bärring and von Storch, 2004; Matulla et al., 2008; Hanna et al., 2008).

In the article **"The Informational Value of Pressure-Based Single-Station Proxies for Storm Activity"** (Krueger and von Storch, 2012) the above mentioned proxies are separately gauged against the 95th and 99th percentile time series of ground-level wind speeds within coastDat to quantify the relation between the pressure-based proxies and storminess. The correlation between high percentiles of ground level wind speeds and the single proxies is used as a measure for the informational value for the proxies. The findings are illustrated in Figure 2.1, which shows the spatial distribution and histograms of the correlations from two proxies as examples. The figure indicates that higher absolute correlations cover the North Atlantic, Scandinavian, Baltic, and the Mediterranean areas, lower values the Central European regions.

TABLE 2.1: The median of the distribution of correlations between several proxies based on pressure readings from single stations (number of pressure observations below 980 hPa N(p < 980 hPa), 1st percentiles of pressure, frequency of absolute pressure tendencies exceeding 25 hPa in 24 h N($|\frac{\Delta p}{\Delta t}| > \frac{25hPa}{24h}$), mean and 99th percentiles of absolute pressure tendencies) and the 95th percentiles of surface wind speeds for the annual time scale (from Krueger and von Storch, 2012).

	median correlation
N(p < 980 hPa)	0.24
1st percentiles of p	-0.26
N($|\frac{\Delta p}{\Delta t}| > \frac{25hPa}{24h}$)	0.23
mean of $|\frac{\Delta p}{\Delta t}|$	0.43
99th percentiles of $|\frac{\Delta p}{\Delta t}|$	0.37

The results demonstrate that the proxies are generally linearly linked to storm activity. The proxies involving absolute pressure tendencies have the highest informational content (see Table 2.1). Nevertheless, the correlations found indicate only weak to moderate informational value. The histograms in Figure 2.1 imply that the number of occurrences of higher absolute correlations is small, owing either to a poor design (that is, the proxies are highly sensitive to chosen thresholds and the measurement frequency) or to the fact that the occurrences of low pressure or high pressure tendencies do not connect with high surface wind speeds directly in space or time.

The article Krueger and von Storch (2012) therefore also examines the question as to whether the proxies have the capability of representing storminess on larger horizontal scales. The results indicate that the correlation with absolute pressure tendencies increases with increasing horizontal scales (Section 3 in Krueger and von Storch, 2012). Absolute pressure tendencies thus can potentially describe storminess over a larger area surrounding a weather station. Low pressure readings do not show such an improvement in general. If land and sea surface conditions are separately taken into account, a considerably improved informational content of low pressure readings reveals itself over sea surfaces on larger horizontal scales only. Overall, the informational value of the examined pressure-proxies is higher over sea than over land surfaces.

A thorough discussion and detailed explanation of the aforementioned findings is presented in "The Informational Value of Pressure-Based Single-Station Proxies for Storm Activity" (Krueger and von Storch, 2012).
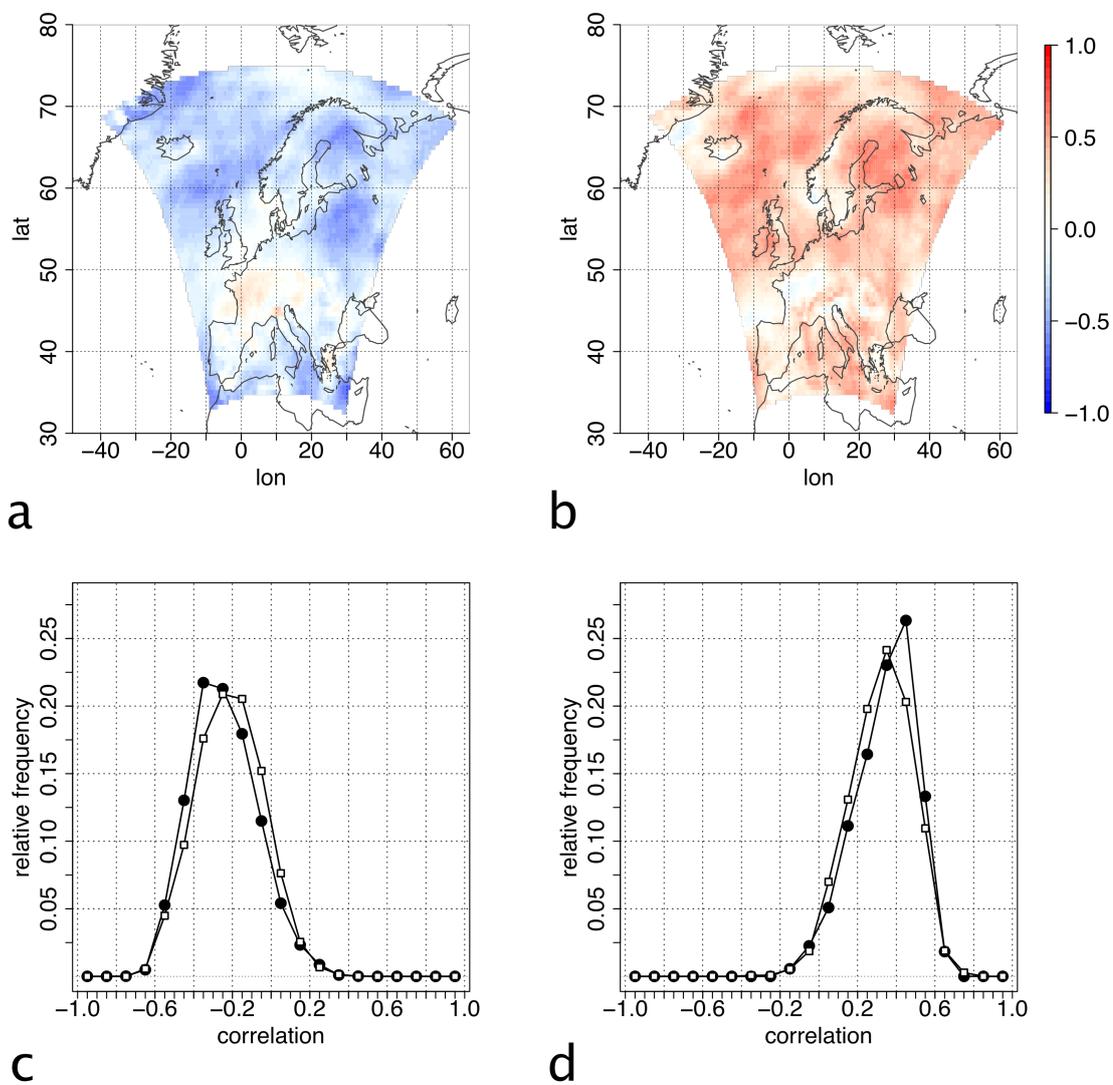
FIGURE 2.1: Spatial distributions of correlations between annual 95th percentiles of surface wind speeds and the annual (a) 1st percentile of pressure readings, and (b) 99th percentiles of absolute pressure tendencies in 24 h. The panels (c) and (d) in the bottom row show the histograms of correlations associated with the proxies in (a) and (b) in the same order. In (c) and (d), the correlation with annual 95th percentiles of surface wind speeds (filled circles) and the correlation with annual 99th percentiles of surface wind speeds (white squares) are shown (from Krueger and von Storch, 2012).

2.2 Statistics of Geostrophic Wind Speeds

Wind speeds in the midlatitudes directly relate to a pressure gradient that determines geostrophic wind speeds. Proxies based on single station readings, on the contrary, seek to detect atmospheric disturbances, which often do not relate to storminess directly. Consequently, it seems advisable to make use of geostrophic wind speeds to build statistics that describe the storm climate within one region. There is one difficulty, however, as pressure observations reaching back long times usually do not cover large areas comprehensively. Determining pressure gradients thus demands spatial interpolation of observed pressure values.

The simplest approach, which has been used for the first time by Schmidt and von Storch (1993), is to use triplets of pressure readings, which represent the corners of triangles, to derive geostrophic wind speeds. Here, three different time series of pressure readings are needed to describe storminess over the area of one triangle independently from measurements within the triangle.[1]

---

[1]The approach by Schmidt and von Storch (1993) interpolates one pressure triplet over the area of one triangle. At each location (x,y) within the triangle, the pressure p is described as

$$p = ax + by + c. \tag{2.1}$$

The coordinates x and y are given by

$$\text{x} = \text{R}_e \lambda \cos(\phi), \tag{2.2}$$
$$\text{y} = \text{R}_e \phi, \tag{2.3}$$

where R_e denotes the Earth radius, λ the longitude, ϕ the latitude. The coefficients a, b, and c in Equation 2.1 are unique for each triangle and can be derived through solving the following set of equations. The station coordinates of the pressure measurements p_1, p_2, and p_3, which form the triangle, are denoted by (x_1, y_1), (x_2, y_2), and (x_3, y_3).

$$\begin{aligned} p_1 &= ax_1 + by_1 + c \\ p_2 &= ax_2 + by_2 + c \\ p_3 &= ax_3 + by_3 + c. \end{aligned} \tag{2.4}$$

The geostrophic wind speed is then calculated as

$$U_{geo} = (u_g^2 + v_g^2)^{1/2}, \tag{2.5}$$

with

$$u_g = -\frac{1}{\rho f}\frac{\partial p}{\partial y} = -\frac{b}{\rho f} \qquad \text{and} \qquad v_g = \frac{1}{\rho f}\frac{\partial p}{\partial x} = \frac{a}{\rho f}, \tag{2.6}$$

where ρ is the density of air (set at 1.25 kg m^{-3}) and f the Coriolis parameter. The coefficients a and b denote the zonal and meridional pressure gradients. Note that f is usually the average of the Coriolis parameter at each measurement site. After having derived U_{geo} at each time step, time series of geostrophic wind speed statistics can be obtained.
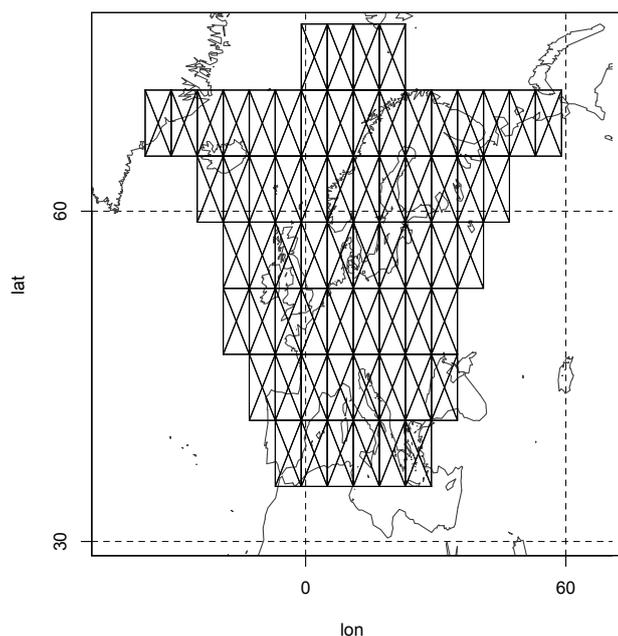
FIGURE 2.2: Illustration of how the REMO model domain (in a $0.5° \times 0.5°$ resolution) has been subdivided into triangles. Here, the length of the sides of the triangles is set to be the distance between 2 points that are 10 grid points apart in the longitudinal and latitudinal direction. These distances range from 1 to 30 grid points in our study. Also, the location of triangles is shifted systematically to maximize the number of possible combinations of such triangles. From this collection of triangles a subset has been chosen randomly that is analyzed in this study (from Krueger and von Storch, 2011).

Schmidt and von Storch (1993) investigated annual frequency distributions of geostrophic wind speeds in the German Bight (North Sea). The authors found no increase in geostrophic storminess concluding that storm activity remained almost constant for the examined period of over 100 years. Later studies (e.g. Schmith, 1995; Alexandersson et al., 1998, 2000; Matulla et al., 2008; Wang et al., 2009), which adopted the method, analyzed geostrophic storminess over the Northeast Atlantic and Europe starting at about 1880. A steep increase in storminess from the 1960s into the 1990s has been repeatedly detected, but based on longer time series of high geostrophic wind speed percentiles, either a negligible or no trend at all could be inferred for Northeast Atlantic and European regions.

The authors of all the above-mentioned studies assumed that any variation in atmospheric wind statistics would be reflected in the geostrophic wind statistics. Or in other words, they assumed that geostrophic and surface wind speed statistics are linearly linked. In the article **"Evaluation of an Air Pressure–Based Proxy for Storm Activity"** (Krueger and von Storch, 2011) we evaluate this assumption. After systematically subdividing the REMO/coastDat domain into triangles of various sizes (Figure 2.2), a randomly chosen subset
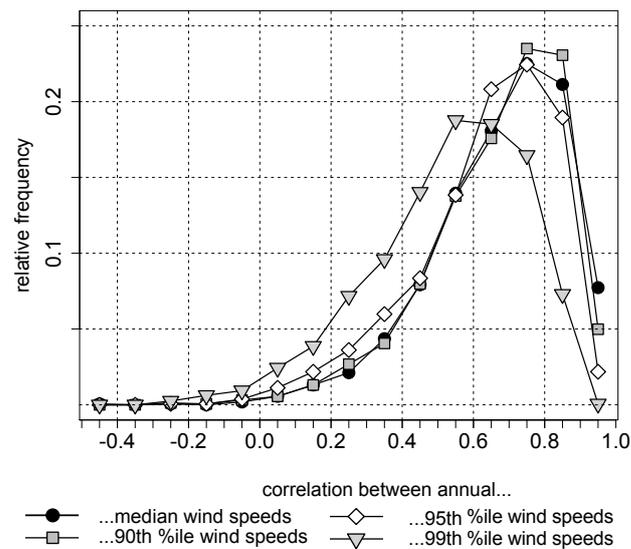
FIGURE 2.3: Histograms of correlations between different annual percentile time series of geostrophic and of area-maximum surface wind speeds (from Krueger and von Storch, 2011).

of triangles is used to determine correlations between the statistics of geostrophic wind speeds and area-maximum ground level wind speeds over the triangles.

In our approach, we compare the median, the 90th, 95th, and 99th annual and seasonal percentiles with each other. Figure 2.3 and Table 2.2 show the histograms and median values of respective annual correlations. The median values that refer to the description of high storminess in Table 2.2 are 0.69 (95th percentiles) and 0.57 (99th percentiles). Together with a formal confirmation of the linear dependence assumption, the found correlations show that describing storminess by use of geostrophic wind speed statistics is skillful. Compared to the obtained correlations for the single-station based proxies (Table 2.1), we see that the informational value of the statistics of geostrophic wind speeds is superior to those of single-station based proxies, as wind speeds in the mid-latitudes directly relate to a pressure gradient that determines geostrophic wind speeds.

Moreover, Krueger and von Storch (2011) also quantify the extent to which different surface conditions and sizes of underlying triangles affect the informational value of geostrophic wind speed statistics (see Table 2.3). For instance, triangles over sea surfaces have on average a correlation that is around 0.21 higher than that of land triangles. Geostrophic wind statistics from sea triangles reflect storm activity better than those from land triangles as the geostrophic wind approximation is less accurate over land, where ageostrophic dynamics, such as frictional influence, play an important role. Further, the mean difference of correlations between small and large triangles is 0.313. Small triangles refer to triangles with an average length of sides of smaller than 300 km, large triangles to those with an average length of sides of equal

TABLE 2.2: The median of the distribution of correlations between different annual percentile time series of geostrophic and of area-maximum surface wind speeds (from Krueger and von Storch, 2011).

Ensembles of correlations between wind speeds	Median
Median	0.718
90th percentiles	0.712
95th percentiles	0.692
99th percentiles	0.573

TABLE 2.3: Inverse-transformed differences in the mean Fisher z correlations for groups of small and large triangles, and land and sea triangles for annual 95th percentiles of geostrophic and surface wind speeds. Small triangles refer to triangles with an average length of sides of smaller than 300 km, large triangles to those with an average length of sides of equal to or greater than 800 km. Medium triangles have an average length of sides in between those values. Land triangles refer to triangles with a land fraction of greater than 0.5, sea triangles to triangles with a land fraction of equal to or less than 0.5 (from Krueger and von Storch, 2011).

Differences in mean correlations	95th percentile wind speeds
Small and large triangles	0.313
Small and medium triangles	0.076
Medium and large triangles	0.242
Sea and land triangles	0.208

to or greater than 800 km. Smaller triangles thus lead to a better description of storminess than larger triangles, due to the fact that larger triangles mask out sharp pressure gradients associated with smaller low pressure systems. Figure 2.4 illustrates the spatial distribution of these findings.

A thorough discussion and detailed explanation of aforementioned points is included in "Evaluation of an Air Pressure–Based Proxy for Storm Activity" (Krueger and von Storch, 2011).
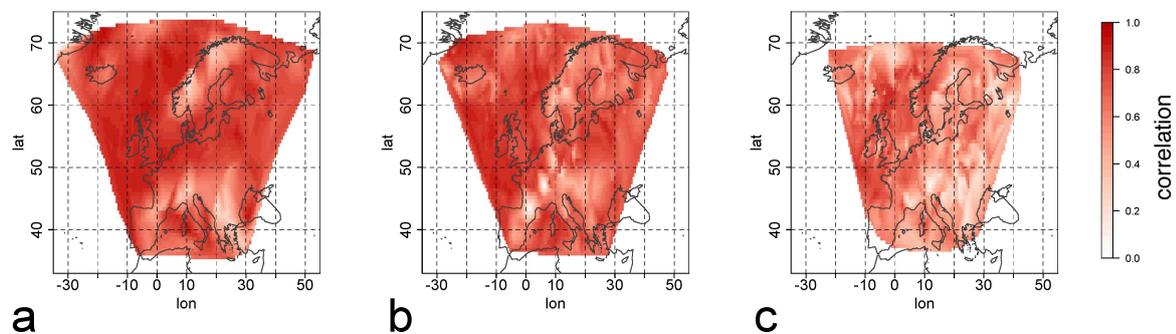
FIGURE 2.4: Spatial distribution of correlations between annual 95th percentile time series of geostrophic and of area-maximum surface wind speeds for (a) small, (b) medium, and (c) large triangles. The spatial distribution of correlations has been obtained by interpolating the correlations bilinearly. Note that small triangles cover a wider area than medium and large triangles because of choosing the examined triangles randomly. In the boundary region, the likelihood of selecting smaller triangles is higher than the likelihood of selecting larger triangles. Note that the same scale is used as in Figure 2.1. (The figure has been taken from Krueger and von Storch (2011).)

2.2.1   A Note on Low-Pass Filtering

In Krueger and von Storch (2011), we also examine the influence of low-pass filtering on the informational content of geostrophic wind speed statistics. Low-pass filtering a time series removes the short-term variability and helps to unmask variability on longer time scales. By comparing low-pass filtered geostrophic wind speed percentile time series with unfiltered ground level area-maximum wind speed statistics, we conclude that "low-pass filtering does not destroy the positive linear relationship between any of the percentile wind speed time series, although it decreases the informative value." This conclusion is only partially correct and needs to be extended, because low-pass filtering will play an important role in the remainder of this doctoral thesis.

The results of Krueger and von Storch (2011) are listed as "Case A" in Table 2.4 and illustrated in Figure 2.5a. To complement these analyses, low-pass filtered geostrophic wind speed percentile time series are now compared with low-pass filtered ground level area-maximum wind speed statistics. The low-pass filter is a Gaussian filter (with σ=2). While the aforementioned results ("Case A" in Table 2.4, Figure 2.5a) concentrate on the ability of low-pass filtered geostrophic wind speed statistics to describe storminess time series, which include short-term variability, the new approach focusses on the link between the time series without high-frequency variability.

The median values of the distribution of correlations between low-pass filtered percentile time series of geostrophic wind speeds and low-pass filtered percentile time series of area-maximum surface wind speeds are notably higher than those in Krueger and von Storch (2011) ("Case B" in Table 2.4). For instance, the median correlation between low-pass filtered annual 95th percentile wind speed statistics increased to 0.831. Also, the distribution of correlations shifted remarkably to higher values (Figure 2.5b). Considering storminess time series on the interannual to interdecadal scale, the findings indicate that low-pass filtering increases the informative value of geostrophic wind speed time series and strengthens the linear link due to the removal of the year-to-year variability.

TABLE 2.4: Case A) Median of the distribution of correlations between low-pass filtered percentile time series of geostrophic and of area-maximum surface wind speeds (as in Krueger and von Storch, 2011), denoted in the table as "cor(LP, noLP)". Case B) Median of the distribution of correlations between low-pass filtered percentile time series of geostrophic wind speeds and low-pass filtered percentile time series of area-maximum surface wind speeds. Denoted in the table as "cor(LP, LP)".

| Ensembles of correlations between wind speed statistics of	Median correlation cor(LP, no LP) (Case A)	Median correlation cor(LP, LP) (Case B)
Median	0.407	0.795
90th percentile	0.464	0.852
95th percentile	0.454	0.831
99th percentile	0.377	0.724
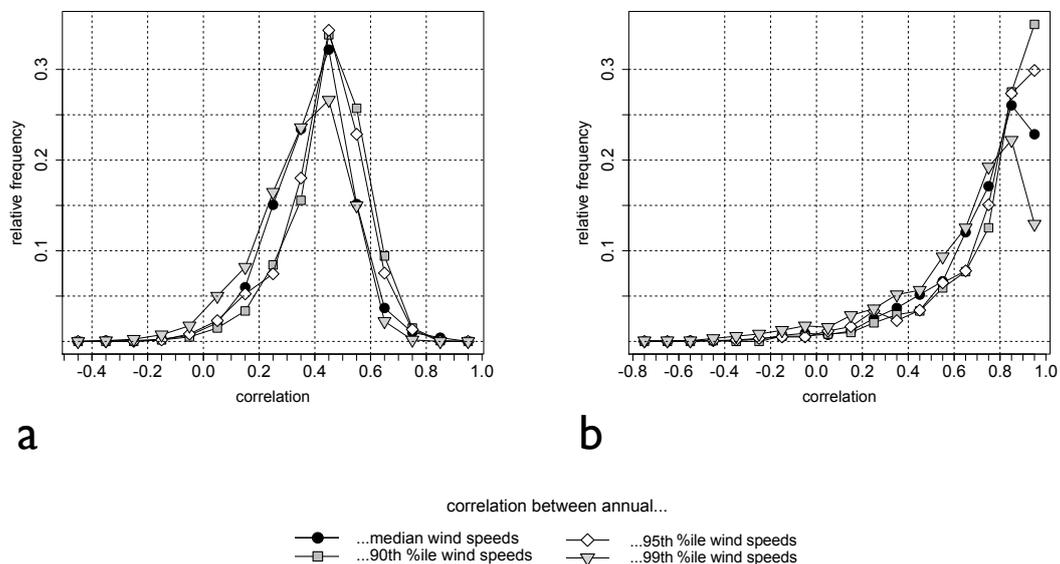
FIGURE 2.5: a) The distribution of correlations between low-pass filtered percentile time series of geostrophic and of area-maximum surface wind speeds (from Krueger and von Storch, 2011). b) The distribution of correlations between low-pass filtered percentile time series of geostrophic wind speeds and low-pass filtered percentile time series of area-maximum surface wind speeds.

3 Inconsistencies between Long-Term Storminess Trends Derived from the Twentieth Century Reanalysis 20CR and Observations

In addition to analyses of past storminess from long time series of observed pressure readings, pressure-based proxies are a useful tool to assess how realistically numerical reanalyses simulate the past storm climate. Numerical reanalyses here refer to retrospective analyses of the state of the atmosphere (or other dynamical systems) with the aid of a numerical model and data assimilation systems. One purpose of reanalyses is to reduce inhomogeneities and irregularities in datasets due to unevenly distributed or inhomogeneous observations (Glickman and Zenk, 2000; Weisse, 2012). As examples for well-known reanalyses, the ERA-40 reanalysis (Uppala et al., 2005) or the NCEP/NCAR reanalysis (Kalnay et al., 1996; Kistler et al., 2001) can be named.

Most reanalyses available cover periods of up to several decades mostly for the second half of the 20th century. While the datasets representative for recent decades might be less affected by inhomogeneities, such records are too short to fully assess natural climate variability and long-term changes. Therefore the 20th Century Reanalysis (20CR) project was established to produce a comprehensive global atmosphere dataset covering the period from 1871 onwards (Compo et al., 2011). By assimilating only surface pressure observations with sea-ice and sea surface temperature anomalies as boundary conditions, it was anticipated that inhomogeneities would be largely reduced, and, furthermore, that the dataset would become a valuable resource for both climate model validations and diagnostic studies (Compo et al., 2011).

In the article **"Inconsistencies between Long-Term Trends in Storminess Derived from the 20CR Reanalysis and Observations"** (Krueger et al., 2013), we focus on the extent to which long-term trends in storm activity over Europe and the Northeast Atlantic may be derived from 20CR. Instead of relying on wind speed measurements themselves, which

15

frequently suffer from inhomogeneities such as changes in measurement techniques, relocation of stations, or changes in the surrounding of stations (e.g. Wan et al., 2010; Lindenberg, 2011), we use a well established proxy for storm activity based on geostrophic wind speeds derived from surface pressure data (see Section 2.2). The index was originally proposed by Schmidt and von Storch (1993) and later on extensively used by other authors (e.g. Alexandersson et al., 2000; Bärring and von Storch, 2004; Matulla et al., 2008; Wang et al., 2009).

In Krueger and von Storch (2011), we showed that the informational content of this proxy is high enough to describe past storminess. Updates of suchlike indices are provided in the IPCC's 4th Assessment report to describe long-term changes and variability of storm activity (Figure 3.41 in Trenberth et al., 2007). Moreover, marine surface pressure measurements are less likely to be affected by inhomogeneities as marine surface pressure represents (compared to near-surface wind speeds) a relatively large-scale variable that is less affected by changes in instrumentation, small relocations of stations, or changes in the surrounding of stations. We also concentrate on an area (the Northeast Atlantic) known to have a relatively high station density throughout the period for which 20CR was performed (Donat et al., 2011) in order to provide a conservative estimate.

The approach in Krueger et al. (2013) follows Alexandersson et al. (1998) and Alexandersson et al. (2000), such that 10 triangles of mean sea level pressure from observations and from 20CR in the Northeast Atlantic (see Figure 3.1) are used to derive long time series of upper annual percentiles of geostrophic wind speeds, which are standardized, averaged, and low-pass filtered. This procedure ensures that the resulting time series is a robust estimate of storminess on a large scale. We repeat the calculations for each of the 56 ensemble members of 20CR and derive an ensemble mean of the storminess time series in 20CR as suggested by Compo et al. (2011). Storminess time series derived from 20CR and from observations can then be compared with each other.

Figure 3.2 shows the resulting time series of low-pass filtered averages of standardized annual 95th percentiles of geostrophic wind speeds. While storminess derived from 20CR (black line) emphasizes an upward trend over the whole period covered, storminess derived from observations (blue line) differs. Except from a decline in the 1880s, a trend over the entire analysis period derived from observations is not visible. Decadal-scale variability dominates the observation-based time series. Both time series differ substantially in the earlier and only agree in the later decades.

In Krueger et al. (2013), we also analyze the 20CR-ensemble standard deviation of the mean sea level pressure and the number of assimilated station readings over the regarded area. The former represents the uncertainty in pressure measurements. It further reflects, to a certain degree, the number (or lack) of assimilated pressure observations over land and sea, which
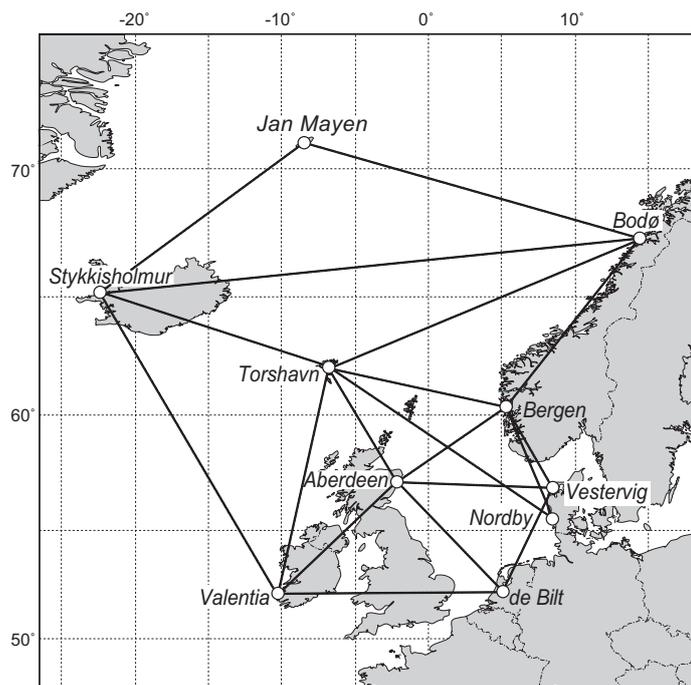
FIGURE 3.1: Pressure observations from various stations have been used to derive geostrophic wind speed time series over 10 triangles over NE Atlantic and European regions (Krueger et al., 2013).

is confirmed by the latter measure. Both measures (presented in Figure 3.3) suggest that the inconsistencies found are most likely caused by the increasing number of observations assimilated into 20CR over time. The inconsistencies are largest during the first half of 20CR when less stations are assimilated and storm activity is surprisingly low. The inconsistencies are already large over a supposedly well monitored region. Our findings suggest that similar problems may arise, in particular over more data-sparse regions. Other studies that assessed different variables and considered different regions within 20CR are in line with our results (Ferguson and Villarini, 2012; Paek and Huang, 2012). For instance, Ferguson and Villarini (2012) recently found inhomogeneities in 20CR air temperature and precipitation which led to their suggestion to restrict climate trend applications over the central United States to the second half century of the 20CR records.

The issue is further explained and elaborated on in "Inconsistencies between Long-Term Trends in Storminess Derived from the 20CR Reanalysis and Observations" (Krueger et al., 2013).
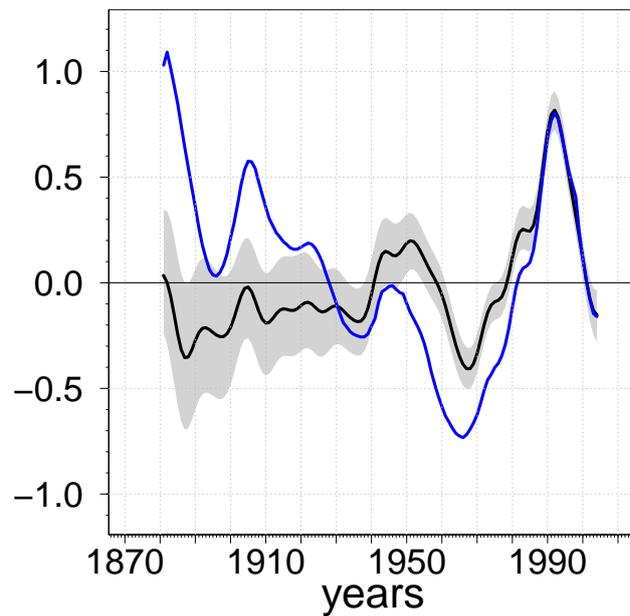
FIGURE 3.2: Standardized time series of annual 95th percentiles of geostrophic wind speeds over 10 triangles in the North Atlantic, which have been averaged and lowpass filtered thereafter. The black line denotes the ensemble mean of these time series in 20CR, along with the complete associated ensemble spread, which is represented by the minimum and maximum values of the ensemble. The blue line is reconstructed after Alexandersson et al. (2000) for the period 1881- 2004 (taken from Krueger et al., 2013).
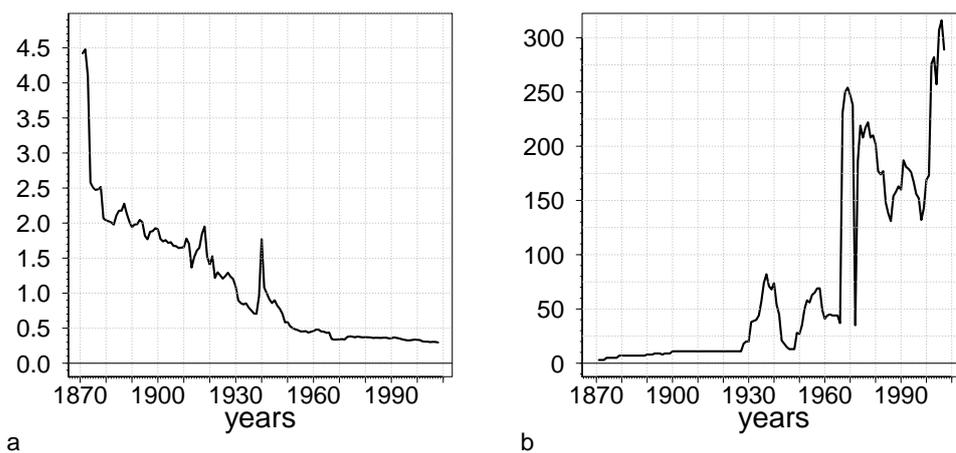
FIGURE 3.3: a) Yearly mean values of the area-averaged 20CR ensemble standard deviation of the surface pressure in hPa. Here, all grid points from 51.9°N to 71°N and from 22.7°W to 14.5°E have been averaged. b) The number of assimilated stations in 20CR from 51.9°N to 71°N and from 22.7°W to 14.5°E, which has been determined from metadata provided by Compo et al. (2011) (taken from Krueger et al., 2013).

4   Outlook

While the previous chapters cover the most important points concerning the informational value of pressure-based proxies for storm activity, other questions that came up in the course of working on this thesis are left unanswered. These questions include the evaluation of other more uncommon pressure-based proxies (for instance, Wavelet-based proxies suggested by Bärring and Fortuniak (2009)), the suitability of pressure proxies in low latitudes (except the geostrophic wind speed), or further in-depth analyses of the representativity of storminess in reanalysis datasets. Apart from these points, other ideas might be more appealing. The following sections present two topics suitable for further research.

4.1   Uncertainties in Pressure Measurements and Robustness of Pressure-Based Proxies

Measurement errors and other sources of uncertainty complicate the evaluation and interpretation of observations and derived quantities. So far, it has not been examined to what extent measurement errors and other uncertainties in pressure observations affect the link between proxy statistics and storminess. Of course, such work would require consistent pressure and wind speed data, for instance from the coastDat dataset. Following the work of Schmith et al. (1997), three general sources of uncertainties in pressure measurements can be considered to influence the link between pressure-based proxy statistics and ground level wind speed statistics. The following three cases address these sources of uncertainty.

First, one should assume normally distributed errors with a mean of 0 and a standard deviation ranging from very small to high values (for instance from 0.01 to 5 hPa), which are added to the pressure values. The chosen range covers the order of uncertainty due to the corrections of different observation hours, temperature, index errors of barometers, height, and dynamical pressure (Schmith et al., 1997). Even though these error sources might be skewed in reality, they can be assumed to be normally distributed in order to generalize all these cases.

In the second case, the analysis should focus on single errors or pressure outliers, which might be caused by digitizing old handwritten pressure records. There is no exact definition of outliers. A common approach to identify outliers is to screen for values farther away than 3 standard deviations from the mean value. This definition also means that outliers occur less than in 1 of 1000 cases or less than 9 times a year (for hourly values). In a possible approach, the outlier error is drawn randomly from a range that covers the outliers (with a random sign) n times in a certain period. Then, these outlier errors are added to n randomly chosen pressure values in that period. It would be better to choose conservatively. That is the outlier range should rather be too high and such errors should be considered rather often to be noticeable in proxy-frequency distributions.

The third case of uncertainty deals with station movements, which is a rather important subject for geostrophic wind speeds. A possible approach would be to change the location of one station randomly by some kilometers multiple times in a certain period. The pressure values would be left unchanged, because the air pressure is a relatively large-scale variable, which does not show high variability on small scales. To make effects of relocations visible, the choice of the distances should be rather high (maybe 10 km). Also, a relative high frequency of relocations would be useful. However, the results might be exaggerated when compared to reality.

For each case, the calculations should be repeated multiple times (perhaps 1000 times) to obtain frequency distributions of the correlation between pressure-based proxy statistics and ground level wind speed statistics. Then, as a measure for the uncertainty of the linear link between both statistics, the interquartile range (a robust nonparametric measure for the dispersion of a frequency distribution) of the correlation could be used. Preliminary analyses for the geostrophic wind speed statistics derived from triangles of surface pressure suggest that the uncertainty of the link scales almost linearly with the uncertainty of observations. Also, outliers seem not to play a significant role. These analyses also show that changes in the station locations within several kilometers may mainly affect smaller triangles.

4.2   The Combination of Pressure-Based Proxies

The different pressure proxies address different aspects of storminess that are related to each other. For instance, the single-station proxies exploit local pressure changes and low pressure values. Geostrophic wind speed statistics from triangles of surface pressure readings make use of large-scale pressure gradients. In principle a combination of all the proxies discussed in this study should provide a proxy with superior informative value compared to that of the individual proxies.

Even though a simple multiple linear regression might be feasible, a multiple regression on the different classes of shared information would be more appealing. Then, redundant information would be discarded and the analysis would concentrate on the unique pieces of shared information among the proxies.

In preliminary analyses within coastDat we applied a principal component analysis (for details see von Storch and Zwiers, 2002) on the proxies examined in this thesis. We found that the first three principal components account for more than 90% explained variance among the proxies. By definition, the principal components are independent from each other. The first principal component accounts for the shared information of all proxies, the second principal component accounts for the information shared among geostrophic wind speed and pressure tendency statistics opposed to low pressure readings, and the third concentrates on geostrophic wind speed statistics. Higher order principal components are structured erratically and only add little information (illustrated in Figure 4.1). While the first principal component accounts for a great amount of variance, a combination of the first three principal components would account for most of the variance among the proxies.
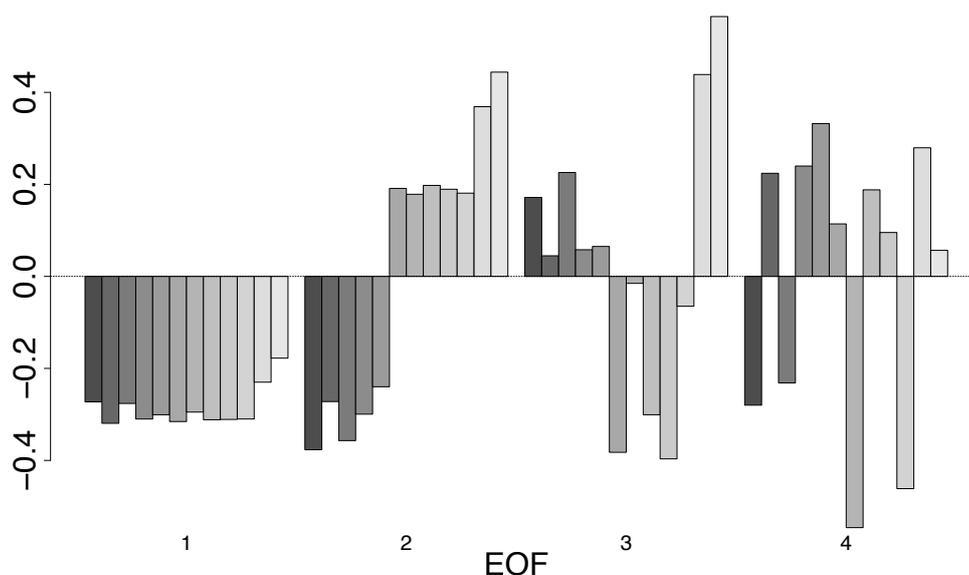
FIGURE 4.1: First four eigenvectors of a principal component analysis of pressure-based proxies at 9.2 °E and 49.4 °N in coastDat. The components of each eigenvector are (from left to right) the first and fifth annual percentiles of the pressure; the annual number of occurrences of pressure readings below the first, fifth, and tenth 60 years percentile; the 95th and 99th annual percentiles of absolute 24 hourly pressure tendencies; the annual number of occurrences of 24 hourly absolute pressure tendencies greater than the 90th, 95th, and 99th 60 years percentile of absolute 24 hourly pressure tendencies; and the 95th and 99th annual percentiles of geostrophic wind speeds (only triangles with an average side length smaller than 300 km) interpolated onto the coastDat domain.

A linear combination or multiple linear regression of the proxies projected onto the three principal components leads to very promising results with a median correlation with ground level wind speed statistics of around 0.6. Figure 4.2 shows the regional distribution of these correlations. Of course, such an approach would mean to fit coefficients in the regression to ground level wind speed statistics, which are usually not available from observations. Also, doing so would be counter-intuitive since pressure proxies are used to describe storminess independently from recorded wind speeds. A possible solution would likely involve regional climate simulations to fit the coefficients and apply them to observations. Such an approach would make it possible to study the regional distribution of coefficients, their dependency on the length of triangle sides, or surface properties. Further research seems warranted.
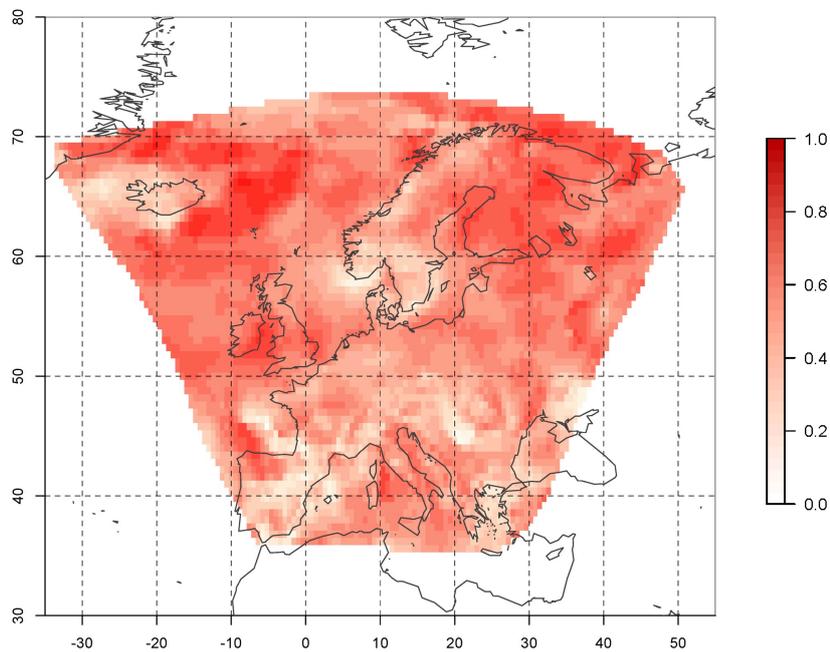

FIGURE 4.2: Correlation between 95th annual percentiles of ground level wind speeds and a linear combination of the first three principal components of 10 different pressure-based proxies (named in Figure 4.1).

5   Conclusions

This thesis presents a systematic evaluation of the informational content of several air pressure-based proxies for storm activity. The two classes of proxies discussed are proxies based on pressure observations from single and multiple stations. The former includes the number of deep lows, lower percentiles of pressure, the frequency of absolute pressure tendencies exceeding certain thresholds, as well as high percentiles and mean values of absolute pressure tendencies. The latter refers to geostrophic wind speed statistics derived from triangles of surface pressure readings. Further, the storm climate within the Twentieth Century Reanalysis (20CR) over the Northeast Atlantic by means of a pressure-based proxy is assessed. Last, two topics suitable for further research are presented. The first topic addresses uncertainties in pressure measurements and their influence on the informational value of pressure-based proxies. The second topic deals with the combination of several pressure-based proxies by using a principal component analysis.

One aim of this thesis was to determine whether the proxies are linked to storminess and to quantify the informational content of the proxies. While all the proxies are generally linked to storminess, results indicate that the statistics of geostrophic wind speeds are a valuable proxy for describing past storm activity and that the other proxies have inferior informative value.

Another aim of this thesis was to consider the influence of surface properties and spatial scales on the proxies' ability of describing storminess. It is found that absolute pressure tendencies can potentially describe storminess over a larger area surrounding a weather station. Low pressure readings can describe storminess on larger horizontal scales over sea. The informative value of geostrophic wind speed statistics deteriorates with increasing triangle size. Overall, the informational value of all the proxies is higher over sea than over land surfaces.

Further, the ability of reproducing the past storm climate over the Northeast Atlantic in 20CR is assessed by comparing 20CR geostrophic wind speed statistics with observation-based geostrophic wind speed statistics. The analyses show that the storm climate in 20CR differs substantially from the storm climate derived from observations in the earlier years until around 1950 due to an increasing number of assimilated pressure observations over time.

Bibliography

Alexander, L., S. Tett, and T. Jonsson, 2005: Recent observed changes in severe storms over the United Kingdom and Iceland. *Geophysical research letters*, **32 (13)**, L13 704.

Alexandersson, H., T. Schmith, K. Iden, and H. Tuomenvirta, 1998: Long-term variations of the storm climate over NW Europe. *The Global Atmosphere and Ocean System*, **6 (2)**, 97–120.

Alexandersson, H., H. Tuomenvirta, T. Schmith, and K. Iden, 2000: Trends of storms in NW Europe derived from an updated pressure data set. *Climate Research*, **14 (1)**, 71–73.

Allan, R., S. Tett, and L. Alexander, 2009: Fluctuations in autumn–winter severe storms over the British Isles: 1920 to present. *International Journal of Climatology*, **29 (3)**, 357–371.

Bärring, L. and K. Fortuniak, 2009: Multi-indices analysis of southern Scandinavian storminess 1780-2005 and links to interdecadal variations in the NW Europe-North Sea region. *International Journal of Climatology*, **29 (3)**, 373–384.

Bärring, L. and H. von Storch, 2004: Scandinavian storminess since about 1800. *Geophys. Res. Lett*, **31**, 1790–1820.

Compo, G., J. Whitaker, P. Sardeshmukh, N. Matsui, R. Allan, X. Yin, B. Gleason, R. Vose, G. Rutledge, P. Bessemoulin, et al., 2011: The twentieth century reanalysis project. *Quarterly Journal of the Royal Meteorological Society*, **137 (654)**, 1–28.

Donat, M., D. Renggli, S. Wild, L. Alexander, G. Leckebusch, and U. Ulbrich, 2011: Reanalysis suggests long-term upward trends in European storminess since 1871. *Geophysical Research Letters*, **38 (14)**, L14 703.

Ferguson, C. R. and G. Villarini, 2012: Detecting inhomogeneities in the Twentieth Century Reanalysis over the central United States. *Journal of Geophysical Research*, **117 (D05123)**, 11.

Feser, F., R. Weisse, and H. von Storch, 2001: Multi-decadal atmospheric modeling for Europe yields multi-purpose data. *Eos*, **82 (28)**, 305.

Glickman, T. and W. Zenk, 2000: *Glossary of Meteorology*. American Meteorological Society.

Hanna, E., J. Cappelen, R. Allan, T. Jónsson, F. Le Blancq, T. Lillington, and K. Hickey, 2008: New insights into North European and North Atlantic surface pressure variability, storminess, and related climatic change since 1830. *Journal of Climate*, **21 (24)**, 6739–6766.

Jonsson, T. and E. Hanna, 2007: A new day-to-day pressure variability index as a proxy of Icelandic storminess and complement to the North Atlantic Oscillation index. *Meteorologische Zeitschrift*, **16 (1)**, 25–36.

Kalnay, E., M. Kanamitsu, R. Kistler, W. Collins, D. Deaven, L. Gandin, M. Iredell, S. Sana, G. White, J. Woollen, et al., 1996: The NCEP/NCAR 40-Year Reanalysis Project. *Bulletin of the American Meteorological Society*, **77**, 437–472.

Kistler, R., E. Kalnay, W. Collins, S. Saha, G. White, J. Woollen, M. Chelliah, W. Ebisuzaki, M. Kanamitsu, V. Kousky, et al., 2001: The NCEP-NCAR 50-year reanalysis: Monthly means CD-ROM and documentation. *Bulletin-American Meteorological Society*, **82 (2)**, 247–268.

Koch, W. and F. Feser, 2006: Relationship between SAR-derived wind vectors and wind at 10-m height represented by a mesoscale model. *Monthly Weather Review*, **134 (5)**, 1505–1517.

Krueger, O., F. Schenk, F. Feser, and R. Weisse, 2013: Inconsistencies between Long-Term Trends in Storminess Derived from the 20CR Reanalysis and Observations. *Journal of Climate*, **26 (3)**, 868–874, doi:10.1175/JCLI-D-12-00309.1.
©American Meteorological Society. Used with permission.
Krueger, O. and H. von Storch, 2011: Evaluation of an Air Pressure–Based Proxy for Storm Activity. *Journal of Climate*, **24 (10)**, 2612–2619.
©American Meteorological Society. Used with permission.
Krueger, O. and H. von Storch, 2012: The Informational Value of Pressure-Based Single-Station Proxies for Storm Activity. *Journal of Atmospheric and Oceanic Technology*, **29 (4)**, 569–580, doi:10.1175/JTECH-D-11-00163.1.
©American Meteorological Society. Used with permission.
Kunz, M., S. Mohr, M. Rauthe, R. Lux, and C. Kottmeier, 2010: Assessment of extreme wind speeds from Regional Climate Models–Part 1: Estimation of return values and their evaluation. *Nat. Hazards Earth Syst. Sci*, **10**, 907–922.

Lindenberg, J., 2011: A verification study and trend analysis of simulated boundary layer wind fields over Europe. Ph.D. dissertation, University of Hamburg, 116 pp.

Matulla, C., M. Hofstätter, I. Auer, R. Böhm, M. Maugeri, H. von Storch, and O. Krueger, 2011: Storminess in Northern Italy and the Adriatic Sea reaching back to 1760. *Physics and Chemistry of the Earth, Parts A/B/C*, **40–41 (0)**, 80 – 85.

Matulla, C., W. Schöner, H. Alexandersson, H. von Storch, and X. Wang, 2008: European storminess: late nineteenth century to present. *Climate Dynamics*, **31 (2)**, 125–130.

Paek, H. and H.-P. Huang, 2012: A Comparison of Decadal-to-Interdecadal Variability and Trend in Reanalysis Datasets Using Atmospheric Angular Momentum. *Journal of Climate*, **25 (13)**, 4750–4758, doi:10.1175/JCLI-D-11-00358.1.

Pinto, J., C. Neuhaus, G. Leckebusch, M. Reyers, and M. Kerschgens, 2010: Estimation of wind storm impacts over Western Germany under future climate conditions using a statistical–dynamical downscaling approach. *Tellus A*, **62 (2)**.

Pryor, S., R. Barthelmie, N. Clausen, M. Drews, N. MacKellar, and E. Kjellström, 2012: Analyses of possible changes in intense and extreme wind speeds over northern Europe under climate change scenarios. *Climate Dynamics*, **38**, 189–208.

Schmidt, H. and H. von Storch, 1993: German Bight storms analysed. *Nature*, **365 (6449)**, 791–791.

Schmith, T., 1995: Occurrence of severe winds in Denmark during the past 100 years. *Proceedings of the sixth international meeting on statistical climatology*, 83–86.

Schmith, T., H. Alexandersson, K. Iden, and H. Tuomenvirta, 1997: North Atlantic-European pressure observations 1868-1995 (WASA dataset version 1.0). Tech. Rep. tr97-3, Danish Meteorological Institute.

Schmith, T., E. Kaas, and T. Li, 1998: Northeast Atlantic winter storminess 1875–1995 re-analysed. *Climate Dynamics*, **14 (7)**, 529–536.

Shepherd, J. and T. Knutson, 2007: The current debate on the linkage between global warming and hurricanes. *Geography Compass*, **1 (1)**, 1.

Trenberth, K., P. Jones, P. Ambenje, R. Bojariu, D. Easterling, A. Klein Tank, D. Parker, F. Rahimzadeh, J. Renwick, M. Rusticucci, et al., 2007: Climate Change 2007: The Physical Science Basis. *Contribution of Working Group I to the Fourth Assessment Report of the Intergovernmental Panel on Climate Change (Cambridge University Press, Cambridge, UK and New York, NY, USA, 2007), Chap. Observations: Surface and Atmospheric Climate Change*, 235.

Uppala, S., P. Kållberg, A. Simmons, U. Andrae, V. Bechtold, M. Fiorino, J. Gibson, J. Haseler, A. Hernandez, G. Kelly, et al., 2005: The ERA-40 re-analysis. *Quarterly Journal of the Royal Meteorological Society*, **131 (612)**, 2961–3012.

von Storch, H. and F. W. Zwiers, 2002: *Statistical Analysis in Climate Research*. 1st ed., Cambridge University Press, Cambridge, UK, 496 pp.

Wan, H., X. L. Wang, and V. R. Swail, 2010: Homogenization and Trend Analysis of Canadian Near-Surface Wind Speeds. *Journal of Climate*, **23 (5)**, 1209–1225, doi:10.1175/2009JCLI3200.1.

Wang, X., F. Zwiers, V. Swail, and Y. Feng, 2009: Trends and variability of storminess in the Northeast Atlantic region, 1874–2007. *Climate Dynamics*, **33 (7)**, 1179–1195.

Weisse, R., 2012: coastDat Glossary. Last checked on 30.08.2012, `http://www.coastdat.de/glossary_overview`, last checked on 30.08.2012.

Weisse, R. and H. von Storch, 2009: *Marine Climate and Climate Change. Storms, Wind Waves and Storm Surges*. Springer Praxis, 219 pp.

Weisse, R., H. von Storch, and F. Feser, 2005: Northeast Atlantic and North Sea storminess as simulated by a regional climate model 1958-2001 and comparison with observations. *J. Climate*, **18 (3)**, 465–479.

Weisse, R., H. von Storch, U. Callies, A. Chrastansky, F. Feser, I. Grabemann, H. Guenther, A. Pluess, T. Stoye, J. Tellkamp, et al., 2009: Regional meteo-marine reanalyses and climate change projections: Results for Northern Europe and potentials for coastal and offshore applications. *Bulletin of the American Meteorological Society*.

List of Publications

This thesis is based upon the following list of publications[1].

- Krueger, O. and H. von Storch, 2011: Evaluation of an Air Pressure–Based Proxy for Storm Activity. Journal of Climate, 24 (10), 2612–2619.

- Krueger, O. and H. von Storch, 2012: The Informational Value of Pressure-Based Single-Station Proxies for Storm Activity. Journal of Atmospheric and Oceanic Technology, 29 (4), 569–580.

- Krueger, O., F. Schenk, F. Feser, and R. Weisse, 2013: Inconsistencies between Long-Term Trends in Storminess Derived from the 20CR Reanalysis and Observations. Journal of Climate, 26 (3), 868-874.

Evaluation of an Air Pressure–Based Proxy for Storm Activity

OLIVER KRUEGER AND HANS VON STORCH

Institute for Coastal Research, Helmholtz-Zentrum Geesthacht, Geesthacht, Germany

ABSTRACT

Yearly percentiles of geostrophic wind speeds serve as a widely used proxy for assessing past storm activity. Here, daily geostrophic wind speeds are derived from a geographical triangle of surface air pressure measurements and are used to build yearly frequency distributions. It is commonly believed, however unproven, that the variation of the statistics of strong geostrophic wind speeds describes the variation of statistics of ground-level wind speeds. This study evaluates this approach by examining the correlation between specific annual (seasonal) percentiles of geostrophic and of area-maximum surface wind speeds to determine whether the two distributions are linearly linked in general.

The analyses rely on bootstrap and binomial hypothesis testing as well as on analysis of variance. Such investigations require long, homogeneous, and physically consistent data. Because such data are barely existent, regional climate model–generated wind and surface air pressure fields in a fine spatial and temporal resolution are used. The chosen regional climate model is the spectrally nudged and NCEP-driven regional model (REMO) that covers Europe and the North Atlantic. Required distributions are determined from diagnostic 10-m and geostrophic wind speed, which is calculated from model air pressure at sea level.

Obtained results show that the variation of strong geostrophic wind speed statistics describes the variation of ground-level wind speed statistics. Annual and seasonal quantiles of geostrophic wind speed and ground-level wind speed are positively linearly related. The influence of low-pass filtering is also considered and found to decrease the quality of the linear link. Moreover, several factors are examined that affect the description of storminess through geostrophic wind speed statistics. Geostrophic wind from sea triangles reflects storm activity better than geostrophic wind from land triangles. Smaller triangles lead to a better description of storminess than bigger triangles.

1. Introduction

Assessing past storm activity is one of the more difficult tasks in climate science. Wind time series are either too short because of lacking observations or are inhomogeneous. Inhomogeneities are caused by observational routines and analyses, type and accuracy of used instruments, the surroundings, and station relocations (Trenberth et al. 2007). As an example for such inhomogeneities the wind time series of Hamburg can be named (Weisse and von Storch 2009). The time series exhibits a decreasing number of days per decade with wind speeds over 7 Beaufort because of the weather station being relocated from the harbor to the airport of Hamburg. Inhomogeneities are also caused by improvements in the observational

framework: with increased supervision of the atmosphere through satellite-based measurements, buoys, and stations came an increased detection rate of storm events that lead to probably false inferences about long-term changes in storminess (Shepherd and Knutson 2007).

Making use of air pressure–based proxies for storm activity, which are based on usually homogeneous pressure readings, is a possible solution to counteract these problems. Several proxies exist, such as the frequency of 24-hourly local pressure changes of 16 hPa or the frequency of pressure readings less than 980 hPa (Bärring and von Storch 2004). Schmidt and von Storch (1993), however, followed a different approach. They investigated geostrophic wind speeds in the German Bight (North Sea). Here, pressure observations from three stations, which form a triangle, were used to calculate geostrophic wind speeds and associated annual frequency distributions. The authors assumed that any variation in atmospheric wind statistics would be reflected in the geostrophic wind statistics. Schmidt and von Storch (1993)

Corresponding author address: Oliver Krueger, Institute for Coastal Research, Helmholtz-Zentrum Geesthacht, Max-Planck-Str. 1, 21502 Geesthacht, Germany.
E-mail: oliver.krueger@hzg.de

found no increase in geostrophic storminess, concluding that storm activity remained almost constant for the examined period of over 100 yr.

In the following years, several studies adopted the method to analyze storminess over different areas in the midlatitudes. A brief technical description of the method can be found in Schmith (1995) and Wang et al. (2009). Alexandersson et al. (1998, 2000) used pressure readings from 21 stations in northwestern Europe and the North Atlantic to form several triangles. They examined the annual 95th and 99th percentiles and found that northwestern Europe storm activity shows interdecadal variability. They also examined the linkage of these percentiles to the North Atlantic Oscillation (NAO) and found that large-scale atmospheric features only moderately explain the long-term behavior of this proxy, mostly because of the assessment of annual distributions. They noted that the correlation between the NAO and winter seasonal percentiles is higher and lower for other seasonal percentile time series. Matulla et al. (2008) updated one of the pressure triangles of Alexandersson et al. (2000) and added further stations over central Europe. They concluded that storminess over central Europe features the same characteristics as storminess over northern Europe. Furthermore, Matulla et al. (2008) stated that the NAO index is not useful in explaining central Europe storm activity. Wang et al. (2009) extended the previous studies using the triangle proxy as they explored seasonal and regional differences in the temporal evolution of northeastern Atlantic storminess. They concluded that storminess in the North Sea region is different to storminess in other regions and that summer and winter storm activity differs. They also found a moderate relationship between winter storminess and the NAO.

The studies that use the triangle proxy commonly assume that the variation of the statistics of strong geostrophic wind speeds describes the variation of statistics of ground-level wind speeds. Although there might be evidence that this assumption is valid (WASA Group 1998; Wang et al. 2009), it is still unproven. The aim of the present study is to close this gap with a systematic evaluation of the triangle pressure proxy. Such an investigation requires long and homogeneous data. Therefore, we use diagnostic 10-m wind and surface air pressure fields from the spectrally nudged and National Centers for Environmental Prediction (NCEP)-driven regional model REMO (Feser et al. 2001; Weisse et al. 2009) for the period 1959–2005. These fields belong to the coastDat dataset (available online at http://www.coastdat.de from the Helmholtz-Zentrum Geesthacht). They used hourly ground-level wind speed and surface air pressure fields over Europe and the North Atlantic with $0.5° \times 0.5°$ resolution (around 50–60 km). Weisse et al. (2005) show

that surface wind fields and their statistics are homogeneous and reasonably well simulated over the sea in coastDat. We assume that the wind fields and their statistics are also reasonably well simulated over land.

The following sections address the evaluation of the triangle pressure proxy for annual and seasonal percentiles. Furthermore, the influence of low-pass filtering, size, and surface properties of underlying triangles on the proxy quality is examined and discussed.

2. Are annual and seasonal percentiles of geostrophic wind speed and of ground-level wind speed positively linearly related?

The assumption that the variation of the statistics of strong geostrophic wind speeds describes the variation of the statistics of ground-level wind speeds implies that percentile time series of geostrophic and of atmospheric wind speed are positively linearly related. To evaluate this assumption, the correlations between specific quantiles of geostrophic and of atmospheric wind speed time series, namely, the median, the 90th, the 95th, and the 99th percentile time series, are investigated. For this purpose we determine annual and seasonal frequency distributions from hourly geostrophic and near-surface wind speeds over various triangles in the dataset region. The triangles are randomly chosen to vary their size and location. In this approach, the length of triangle sides ranges from about 50 to 1800 km (Fig. 1). Over these triangles, geostrophic wind speeds are expected to represent area-averaged wind conditions. For our evaluation, however, we use statistics of area-maximum (instead of area-average) surface wind speeds as a measure of storm activity, which is characterized by strong surface wind speeds. With this choice we set a higher standard for determining a positive link between the statistics of geostrophic wind speeds and storm activity. Note that the usage of statistics of area-averaged wind speeds would result in higher correlations.

Here, 1221 triangles have been examined to assess the correlation between annual time series. Figure 2 displays histograms of the ensemble of correlations between the median, 90th, 95th, and 99th percentile time series of geostrophic and of modeled ground-level wind speeds. Table 1 shows the applicable 0.05 quantiles and the median correlation. The 0.05 quantiles of the four ensembles of correlations are greater than 0. The differences between median correlations of the median, 90th, and 95th percentile time series are small as the values range from 0.692 to 0.718, only the 99th percentile time series have a smaller median correlation of 0.573. From Fig. 2 and the median values of the ensemble of correlations we infer that the median geostrophic wind speed best reflects the variations of annual
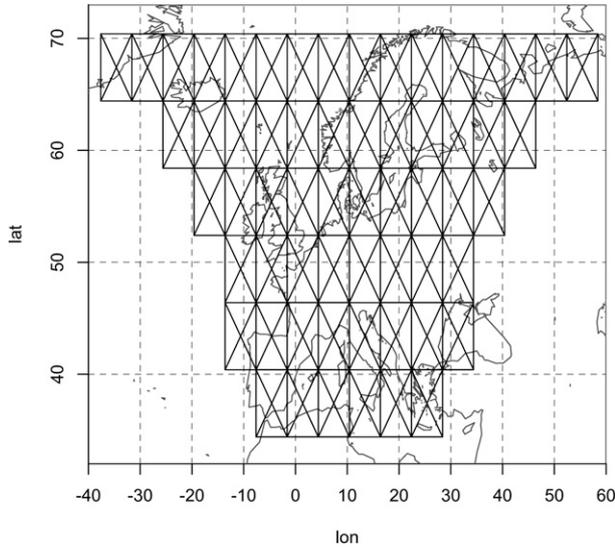
FIG. 1. Illustration of how the REMO model domain (with 0.5° × 0.5° resolution) has been subdivided into triangles. Here, the length of the sides of the triangles is set to be the distance between 2 points that are 10 grid points apart in the longitudinal and latitudinal direction. These distances range from 1 to 30 grid points in our study. Also, the location of triangles is shifted systematically to maximize the number of possible combinations of such triangles. From this collection of triangles a subset has been chosen randomly that is analyzed in this study.

FIG. 2. Histograms of correlations between different percentile time series of geostrophic and of area-maximum surface wind speeds.

ground-level wind speed statistics and that the correlations decrease for upper-quantile time series.

After having derived the percentile time series and respective correlations, the mentioned research question is dealt with in two steps. First, every single correlation is tested locally for a positive linear dependency at the 0.01 significance level via bootstrap hypothesis testing. The proportion h of accepted local null hypotheses given in Table 1 increases for upper-percentile wind time series from about 3.85% (median wind speeds) to 16.95% (99th percentile wind speeds).

Second, these proportions are used to determine a general answer to our question. If quantiles of geostrophic wind speed and of area-maximum wind speed were independent (for instance, would not covary linearly), one would expect $r = 99\%$ of all the sample correlations not to be 0.01 significant on average, and only 1% to be inconsistent with the null hypothesis of a 0 correlation. The likelihood of obtained proportions can be deduced from the binomial distribution (e.g., Livezey and Chen 1983) under this claim, which serves as a global null hypothesis, after the following problem has been addressed.

The results of the first step are not directly applicable to the claim as the percentile time series of different triangles probably depend on each other. Thus, the number of spatially independent time series is likely to be small compared
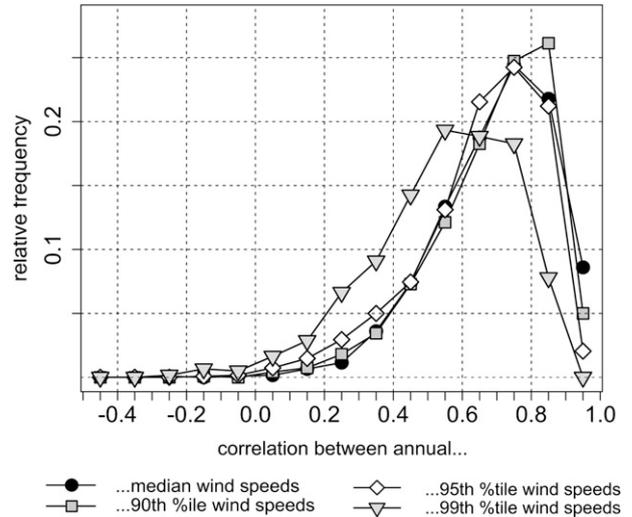
to the number of examined triangles. Different methods suggested in Van den Dool (2007, chap. 6) reveal that the number of spatial degrees of freedom is somewhere between 9 and 25 in our case. For the present study, $N = 20$ spatial degrees of freedom are assumed.

Now, the likelihood of obtained h under the null hypothesis of $r = 99\%$ of all the correlations being 0 in general can be calculated as the cumulative probability of the binomial distribution $P(h \cdot N, N, r)$. Note that the product $h \cdot N$ is rounded as the binomial distribution requires $h \cdot N$ to be an integer number. Our analysis reveals that it would be highly unlikely to achieve the proportions of accepted local null hypotheses if the global null hypothesis was true. The probabilities are in the range of $P \sim 10^{-15}$. Even if h was 80% the probability would be insignificant. These results are in agreement with Fig. 3 in Livezey and Chen (1983). Thus, the global null hypothesis is rejected. The probability that the statement of all the correlations being 0 is valid is extremely low. We conclude that annual percentiles of geostrophic wind speed and of area-maximum wind speed are positively linearly related in general.

TABLE 1. The 0.05 quantile and median of the distribution of correlations between different percentile time series of geostrophic and of area-maximum surface wind speeds. Also shown is the proportion h of accepted local null hypotheses at the 0.01 significance level.

Ensembles of correlations between wind speeds	0.05 quantile	Median	h (%)
Median	0.381	0.718	3.85
90th percentile	0.352	0.712	5.00
95th percentile	0.283	0.692	7.78
99th percentile	0.176	0.573	16.95

TABLE 2. The 0.05 quantile and median of the distribution of correlations between different percentile time series of geostrophic and of area-maximum surface wind speeds for the spring [March–May (MAM)], summer [June–August (JJA)], autumn [September–November (SON)], and winter [December–February (DJF)] seasons. Also shown is the proportion h of accepted local null hypotheses at the 0.01 significance level.

Ensembles of correlations between wind speeds	MAM			JJA			SON			DJF		
	0.05 quantile	Median	h (%)	0.05 quantile	Median	h (%)	0.05 quantile	Median	h (%)	0.05 quantile	Median	h (%)
Median	0.301	0.694	0.93	0.206	0.671	3.70	0.399	0.726	0.77	0.478	0.781	0.62
90th percentile	0.298	0.697	1.85	0.171	0.651	4.78	0.266	0.693	2.16	0.295	0.749	1.54
95th percentile	0.250	0.650	2.77	0.159	0.615	4.94	0.233	0.665	2.78	0.249	0.713	2.78
99th percentile	0.140	0.527	6.48	0.088	0.525	8.64	0.116	0.565	8.79	0.125	0.611	5.40

For seasonal quantiles of geostrophic wind speed and of ground-level wind speed, the same analysis has been carried out for every season. The results are presented in Table 2. Compared with the results of annual percentile time series, the same conclusions can be drawn. There is a linear link between seasonal percentiles of geostrophic wind speed and of area-maximum surface wind speed. Furthermore, the median correlations are between 0.525 and 0.781. They are highest for the winter and lowest for the summer season owing to the seasonal variability of the westerlies. The median correlations decrease for upper percentiles within each season. The differences to the annual median correlations are little. The proportions of accepted local hypothesis tests are smaller than those of the annual results. Consequently, the positive linear relationship also exists on the seasonal scale.

In the literature, storm activity on the interannual-to-interdecadal scale is commonly assessed through low-pass-filtered time series to remove higher-frequency variability. Low-pass filtering, however, certainly affects the linear link between percentile time series; to what extent will be addressed as follows. Now, the analysis has been repeated with a Gaussian filter, whose weights depend on the standard deviation σ (see von Storch and Zwiers 2002, chap. 2, 17). The filter has been applied to the annual geostrophic percentile time series with $\sigma = 2$ prior to calculating the correlations. Low-pass filtering of geostrophic wind quantiles decreases the quality of the linear link, which can be seen in Fig. 3 and Table 3. While unfiltered percentiles mostly show moderate to strong positive linear relationships, low-pass filtering results in weak to moderate linear relationships. The 0.05 quantile of the correlations for the 99th percentiles is just above 0 with a value of 0.053. The proportions of accepted local hypothesis tests are higher (up to 44.96%) than those of unfiltered time series. However, it can be concluded that low-pass filtering does not destroy the positive linear relationship between any of the percentile wind speed time series, although it decreases the informative value.

We have obtained all the results through simulated winds in the virtual world of the regional model REMO. As the statistics of atmospheric wind speeds are reasonable well simulated over sea (Weisse et al. 2005), we expect that the positive linear relationship between variations of the statistics of geostrophic and of ground-level wind speeds
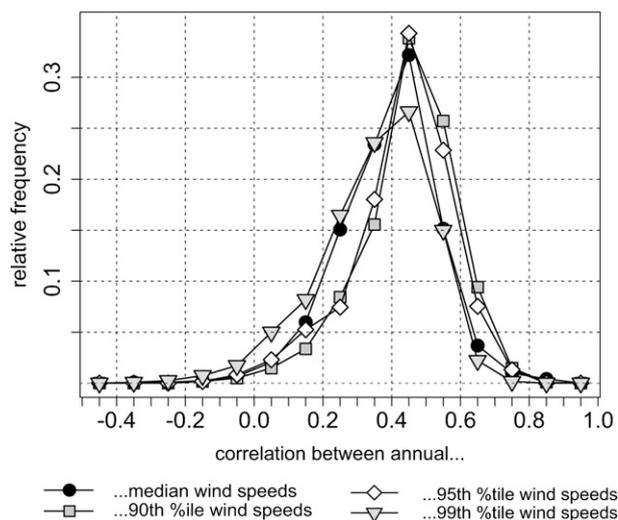
FIG. 3. Histograms of correlations between low-pass-filtered percentile time series of geostrophic and of area-maximum surface wind speeds.

TABLE 3. The 0.05 quantile and median of the distribution of correlations between low-pass-filtered percentile time series of geostrophic and of area-maximum surface wind speeds. The last column denotes the proportion h of accepted local null hypotheses at the 0.01 significance level.

Ensembles of low-pass-filtered correlations between wind speeds	0.05 quantile	Median	h (%)
Median	0.129	0.407	35.54
90th percentile	0.191	0.464	22.03
95th percentile	0.147	0.454	24.90
99th percentile	0.053	0.377	44.96

TABLE 4. Inverse-transformed differences in the mean Fisher z correlations for groups of small and large triangles. Also shown are the inverse-transformed differences for groups of land and sea triangles. The differences are significant at the 0.01 significance level in a Fisher z t test.

Differences in mean correlations	Median wind speeds	90th percentile wind speeds	95th percentile wind speeds	99th percentile wind speeds
Small and large triangles	0.483	0.326	0.313	0.300
Small and medium triangles	0.244	0.086	0.076	0.072
Medium and large triangles	0.271	0.247	0.242	0.233
Sea and land triangles	0.207	0.199	0.208	0.165

also exists in the real atmosphere; to what extent cannot be estimated owing to a lack of observations.

3. How do size and surface conditions influence the description of storm activity?

Wang et al. (2009) noted that the configuration of triangles seems to be important as spatial gradients and differences might be masked out over long distances. To examine whether the configuration of the triangles plays an important role a two-way analysis of variance (ANOVA, e.g., von Storch and Zwiers 2002, chap. 9) has been carried out. We use ANOVA to evaluate the effects of different levels of size and surface conditions on the annual correlation. Furthermore a potential interaction between size and surface conditions is assessed that could emerge for smaller triangles with mixed surface conditions, that is, the two factors may act together on the annual correlation in a different way than they would separately. For that reason, we classify the transformed correlations by different levels of size and surface conditions. Equal group sizes are achieved by collapsing the annual correlations into groups of 116 randomly chosen values.

The response variable is the Fisher z–transformed annual correlation between quantile time series of geostrophic and of area-maximum surface wind speed. The Fisher z transformation is used to obtain a more normally distributed variable to analyze (e.g., von Storch and Zwiers 2002, chap. 8). Explanatory variables are the average length of triangle sides, here referred to as size, and the surface condition, that is, the land fraction, of underlying triangles. The surface condition is classified as land for a land fraction of greater than 0.5 and as sea for a land fraction of equal to or smaller than 0.5.

The size is divided into three groups—smaller than 300 km (small), equal to or greater than 300 km and smaller than 800 km (medium), and equal to or greater than 800 km (large). These classes are chosen for the following two reasons. The characteristic horizontal range of cold fronts stretches from 80 to 300 km (Carlson 1991). Cold fronts that bring a transition from warmer to colder air masses are often accompanied by strong winds. Whether the proxy is capable of detecting such circumstances will be

seen by high correlations between the annual quantile time series. On the other hand, 800 km as the lower boundary for larger-sized triangles mark the transition from mesoscale to synoptic scale atmospheric motions—a characteristic dimension of extratropical cyclones.

The ANOVA, conducted at the 0.01 significance level, reveals that the effects of size and surface conditions on mean Fisher z–transformed correlations are independent among each other. Furthermore, there is a significant difference between the mean Fisher z–transformed correlations because of the surface conditions and size of underlying triangles. For further details on the ANOVA, see the appendix.

Table 4 reveals the inverse-transformed differences in the mean Fisher z–transformed annual correlation for different percentile time series and effects. Figure 4 illustrates the findings for the percentile time series. All the differences are significant at the 0.01 significance level in a Fisher z t test. We have found that geostrophic
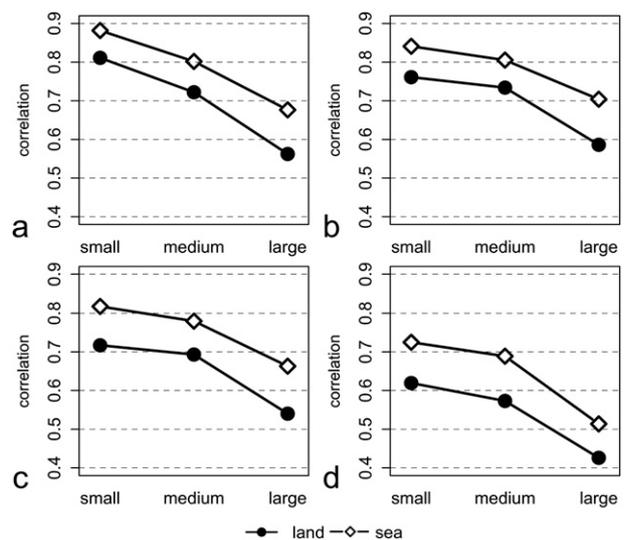
FIG. 4. Inverse-transformed group means of Fisher z–transformed correlations for (a) median, (b) 90th percentile, (c) 95th percentile, and (d) 99th percentile wind speed time series. Shown are the group means for land and sea triangles, as well as small-, medium-, and large-sized triangles.
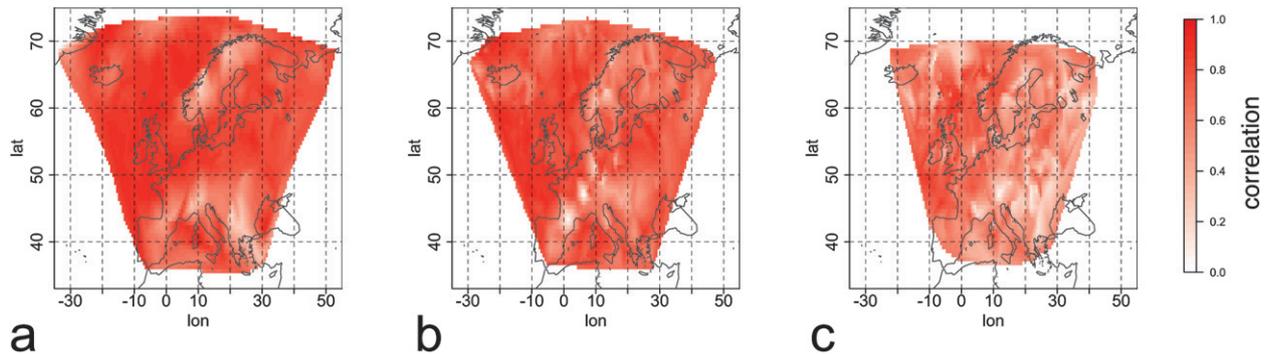
FIG. 5. Spatial distribution of correlations between annual 95th percentile time series of geostrophic and of area-maximum surface wind speeds for (a) small, (b) medium, and (c) large triangles. The spatial distribution of correlations has been obtained by interpolating the correlations bilinearly. Note that small triangles cover a wider area than medium and large triangles because of choosing the examined triangles randomly. In the boundary region, the likelihood of selecting smaller triangles is higher than the likelihood of selecting bigger triangles.

wind from sea triangles reflects storm activity better than geostrophic wind from land triangles. Moreover, smaller triangles lead to a better description of storminess than bigger triangles. The differences in the mean correlations due to size are most distinct with values greater than 0.30 for comparing small and large triangles. The differences, on the contrary, become small between small and medium-sized triangles with values from 0.07 to 0.24. The mean correlations between medium and large triangles differ from 0.23 to 0.27. The effects of surface properties result in differences of about 0.17–0.21. In general the differences are more distinct for the median wind time series and become smaller for upper-percentile wind time series (Table 4).

The higher mean correlation of sea triangles is understandable with regard to turbulent impacts over land that affect surface winds in the planetary boundary layer. The geostrophic wind approximation is less accurate in this layer over land where ageostrophic dynamics play an important role. Over sea the frictional influence from the surface diminishes resulting in a better description of wind speeds through geostrophic wind speeds. Note that these effects strongly depend on the parameterization in the REMO model. The near-surface winds in the model are affected by atmospheric stability and frictional effects of vegetation cover and topography (Jacob and Podzun 1997). The influence of these parameters on the wind is restricted by the spatial resolution in the model, such that turbulence is not described on the subgrid scale in itself. Instead such effects are parameterized. We can only speculate whether a more advanced parameterization would make the differences in the mean correlations due to surface conditions more distinct.

While the differences in the mean correlations between land and sea triangles are in the range of 0.17–0.21, the

differences due to the size are greater and in the range of 0.07–0.48. For all the percentile time series the correlation is highest for small triangles. In contrast to large triangles that mask out pressure gradients, smaller triangles detect small-scale variations. Sharp pressure gradients associated with smaller low pressure systems can be named as examples. The detection of small-scale variations leads to a better description of wind and storm activity. The correlation appears to be also affected by topographical versatility within the triangles, which can be seen in Fig. 5. Figure 5 shows the spatial distribution of the correlation between the annual 95th percentile time series of geostrophic and area-maximum surface wind speed for each triangle size. Whereas the correlations of small triangles only decrease over smaller topographically versatile areas such as the Alps (with values of about 0.2–0.4), the correlations of medium and large triangles are lower than those of small triangles over land in general. Furthermore, the high correlations of smaller triangles are likely to be an effect of the hourly temporal resolution. Small and fast moving low pressure systems are noticed because of the high sampling frequency. Otherwise, these pressure systems would have rushed through the triangles without being recognized. Note that the high correlations of small triangles could also be caused by the regional model REMO that produced the initial data. Its spatial resolution is around 50 km, which is in the range of the smallest triangle size. It could be argued that ageostrophic components of the wind are homogeneously simulated on this spatial scale because of the parameterization, thus making the small-scale wind agree more with the geostrophic wind. A slight indication for this is shown in Table 4, where the differences in the mean correlation between small- and medium-sized triangles are smaller than the differences between other groups of sizes.

4. Concluding remarks

This study aims at a systematic evaluation of the triangle pressure proxy that has been and will be used to assess past and recent storm activity in the midlatitudes. Results obtained from examining the correlation between specific percentile time series of geostrophic wind speed and of area-maximum surface wind speed over various triangles show that the variation of strong geostrophic wind speed statistics describes the variation of ground-level wind speed statistics. Even though we used area-maximum (instead of area-averaged) surface wind speeds, we could show that annual and seasonal quantiles of geostrophic wind speed and of ground-level wind speed are positively linearly related. We verified the linear link by using simulated air pressure and ground-level wind speed in a regional model. We expect that the linear relationship as well exists in the real atmosphere as it does in the simulation. We also considered the influence of low-pass filtering, which decreases the quality of the linear link. Furthermore, we examined several factors that affect the description of storminess through geostrophic wind speed statistics. Geostrophic wind from sea triangles reflects storm activity better than geostrophic wind from land triangles. Smaller triangles lead to a better description of storminess than bigger triangles.

APPENDIX

Application of a Two-Way ANOVA

The general idea of analysis of variance (ANOVA) is to decompose the variability in the response variable among different factors (e.g., von Storch and Zwiers 2002, chap. 9). If the factors produce a significant amount of variation in the response variable, they will result in different mean values (in the categorized response variable). In our study we make use of a two-way ANOVA that also allows us to assess combined effects of the factors. In that case, the influence on the response variable is not independent among the involved factors. If two factors act independently of each other, the contribution made by any one of them is through the values of its individual levels, regardless of the level of the other factor.

The two-way analysis of variance helps us to determine whether the variation of the response variable, in our case the Fisher z–transformed annual correlation, is due

to known causes, which are the factors size and surface conditions of underlying triangles, or whether it is due to random, unexplained causes.

The used factorial model of the ANOVA reads

$$Y_{ijk} = \mu + \alpha_i + \beta_j + (\alpha\beta)_{ij} + \epsilon_{ijk}, \qquad (A1)$$

where Y_{ijk} denotes the kth Fisher z–transformed annual correlation (with $k = 1, \ldots, 116$) in the (ij)th combination of size and surface conditions, where $i = 1, 2, 3$ (respectively small, medium, or large) and $j = 1, 2$ (land or sea). Here, μ is the overall mean Fisher z–transformed annual correlation, α_i is the effect of the size, and β_j is the effect of surface conditions on the transformed correlation. Also, $(\alpha\beta)_{ij}$ is the effect on the correlation when different levels i and j of size and surface conditions are combined, which indicates the effect of interaction between size and surface conditions, and ϵ_{ijk} represents the random effect on the (ijk)th transformed correlation and is assumed to be a zero mean and normally distributed variable with variance σ_ϵ^2.

The ANOVA is carried out with three null hypotheses: two hypotheses for the direct (main) effects and one for the combined effect on the correlation. The first (second) main effect null hypothesis H_0 states that there is no difference between the mean Fisher z–transformed correlations due to surface conditions (due to size of triangles), and alternative hypothesis H_1 that there is a difference due to surface conditions (due to size of triangles). The interaction null hypothesis H_0 declares that there is no interaction between the size of triangles and the surface conditions, the effects of size and surface conditions are independent. Its alternative hypothesis H_1 denotes the existence of an interaction between the size and the surface conditions. The effects of size, in that case, depend on the surface conditions and vice versa.

The ANOVA requires several assumptions that need to be taken care of. Every Fisher z–transformed annual correlation in the (ij)th combination of size and surface conditions is assumed to be normally distributed with equal variance. The validity of the first assumption has been tested by using a Kolmogorov–Smirnov test, the latter one by a χ^2 test. Both tests have been performed at the 0.05 significance level. Further, the ANOVA requires the transformed correlation in the (ij)th combination of factors to be independent, which we have considered by selecting the sample randomly.

Under H_0 the test statistic, the ratio VR $= \sigma^2/\sigma_\epsilon^2$ between explained and unexplained variance in the sample, follows a central F distribution with two different degrees of freedom ϑ. VR, which is estimated from the sample for each of the two factors and their combination, is used to calculate the probability value $P(\text{VR} > F_{\vartheta, \vartheta_\epsilon, \text{VR}})$. Here, P

TABLE A1. Degrees of freedom ϑ, variance σ^2, and variance ratio between explained and unexplained variance (VR) for each source of variation in a two-way analysis of variance of Fisher z–transformed correlations between annual 95th percentiles of geostrophic and of area-maximum surface wind speeds. Under H_0, P determines the probability value to find a VR that is at least as extreme as the calculated variance ratio. The sources of variation are the factors size α, surface condition β, their combination $(\alpha\beta)$, and the random error components ϵ.

Source of variation	ϑ	σ^2	VR $= \sigma^2/\sigma_\epsilon^2$	$P(\text{VR} > F_{\vartheta, \vartheta_\epsilon, \text{VR}})$
α	2	6.669	78.546	$\sim 10^{-16}$
β	1	7.727	91.007	$\sim 10^{-16}$
$\alpha\beta$	2	0.060	0.711	0.446
ϵ	690	0.085	—	—

determines the probability to find a variance ratio VR that is at least as extreme as the calculated variance ratio; H_0 is thus accepted (rejected) when P is greater (smaller) than the used significance level.

The degrees of freedom and the test statistics are presented in Table A1 for the Fisher z–transformed correlations between the annual 95th percentile wind speed time series. For the other wind speed time series the values of the test statistics differ but the same conclusions can be drawn.

The ANOVA accepts the interaction null hypothesis at the 0.01 significance level. The effects of size and surface conditions on mean Fisher z–transformed correlations are independent. Furthermore, the other two null hypotheses are rejected at the 0.01 significance level. Thus, there is a significant difference between the mean Fisher z–transformed correlations owing to the surface conditions and size of underlying triangles.

REFERENCES

Alexandersson, H., T. Schmith, K. Iden, and H. Tuomenvirta, 1998: Long-term variations of the storm climate over NW Europe. *Global Atmos. Ocean Syst.,* **6,** 97–120.

——, H. Tuomenvirta, T. Schmith, and K. Iden, 2000: Trends of storms in NW Europe derived from an updated pressure data set. *Climate Res.,* **14,** 71–73.

Bärring, L., and H. von Storch, 2004: Scandinavian storminess since about 1800. *Geophys. Res. Lett.,* **31,** 1790–1820.

Carlson, T. N., 1991: *Mid-Latitude Weather Systems.* Harper Collins Academic, 507 pp.

Feser, F., R. Weisse, and H. von Storch, 2001: Multi-decadal atmospheric modeling for Europe yields multi-purpose data. *Eos, Trans. Amer. Geophys. Union,* **82,** 305.

Jacob, D., and R. Podzun, 1997: Sensitivity studies with the regional climate model REMO. *Meteor. Atmos. Phys.,* **63,** 119–129.

Livezey, R., and W. Chen, 1983: Statistical field significance and its determination by monte carlo techniques. *Mon. Wea. Rev.,* **111,** 46–59.

Matula, C., W. Schöner, H. Alexandersson, H. von Storch, and X. Wang, 2008: European storminess: Late nineteenth century to present. *Climate Dyn.,* **31,** 125–130.

Schmidt, H., and H. von Storch, 1993: German Bight storms analysed. *Nature,* **365,** 791.

Schmith, T., 1995: Occurrence of severe winds in Denmark during the past 100 years. *Proc. Sixth Int. Meeting on Statistical Climatology,* Galway, Ireland, All-Ireland Statistics Committee and Cosponsors, 83–86.

Shepherd, J., and T. Knutson, 2007: The current debate on the linkage between global warming and hurricanes. *Geogr. Compass,* **1,** 1.

Trenberth, K. E., and Coauthors, 2007: Observations: Surface and atmospheric climate change. *Climate Change 2007: The Physical Science Basis,* S. Solomon et al., Eds., Cambridge University Press, 235–336.

Van den Dool, H., 2007: *Empirical Methods in Short-Term Climate Prediction.* Oxford University Press, 240 pp.

von Storch, H., and F. W. Zwiers, 2002: *Statistical Analysis in Climate Research.* 1st ed. Cambridge University Press, 496 pp.

Wang, X., F. Zwiers, V. Swail, and Y. Feng, 2009: Trends and variability of storminess in the Northeast Atlantic region, 1874–2007. *Climate Dyn.,* **33,** 1179–1195.

WASA Group, 1998: Changing waves and storms in the Northeast Atlantic? *Bull. Amer. Meteor. Soc.,* **79,** 741–760.

Weisse, R., and H. von Storch, 2009: *Marine Climate and Climate Change: Storms, Wind Waves and Storm Surges.* 1st ed. Springer Praxis Environmental Sciences Series, Vol. 4109, Springer, 200 pp.

——, ——, and F. Feser, 2005: Northeast Atlantic and North Sea storminess as simulated by a regional climate model 1958–2001 and comparison with observations. *J. Climate,* **18,** 465–479.

——, and Coauthors, 2009: Regional meteorological–marine reanalyses and climate change projections: Results for Northern Europe and potentials for coastal and offshore applications. *Bull. Amer. Meteor. Soc.,* **90,** 849–860.

The Informational Value of Pressure-Based Single-Station Proxies for Storm Activity

OLIVER KRUEGER AND HANS VON STORCH

Institute for Coastal Research, Helmholtz-Zentrum Geesthacht, Geesthacht, Germany

ABSTRACT

Air pressure readings and their variations are commonly used to make inferences about storm activity. More precisely, it is assumed that the variation of annual and seasonal statistics of several pressure-based proxies describes changes in the past storm climate qualitatively, an assumption that has yet to be proven.

A systematic evaluation of the informational content of five pressure-based proxies for storm activity based on single-station observations of air pressure is presented. The number of deep lows, lower percentiles of pressure, the frequency of absolute pressure tendencies above certain thresholds, as well as mean values and high percentiles of absolute pressure tendencies is examined. Such an evaluation needs long and homogeneous records of wind speed, something that is not available from observations. Consequently, the proxies are examined by using datasets of ground-level wind speeds and air pressure from the NCEP-driven and spectrally nudged regional model, REMO. The proxies are gauged against the 95th and 99th percentile time series of ground-level wind speeds to quantify the relation between pressure-based proxies and storminess. These analyses rely on bootstrap and binomial hypothesis testing. The analyses of single-station-based proxies indicate that the proxies are generally linearly linked to storm activity, and that absolute pressure tendencies have the highest informational content. Further, it is investigated as to whether the proxies have the potential for describing storminess over larger areas, also with regard to surface conditions. It is found that absolute pressure tendencies have improved informational value when describing storm activity over larger areas, while low pressure readings do not show improved informational value.

1. Introduction

When it comes to past observations of wind, researchers face problems that make the assessment of storm activity very difficult. Because changes in storminess affect ecosystems and living conditions, the evaluation of the past storm climate provides valuable knowledge for people, countries, or even more profit-orientated entities, such as insurance companies or the wind energy industry. However, time series of observed wind are mostly too short and inhomogeneous to evaluate past storm activity objectively. Changes in instruments used, sampling routines, the surrounding environments, or the location of weather stations almost always cause inhomogeneities (Trenberth et al. 2007). For instance, the recorded wind speed time series from the island of Helgoland located in the German Bight has been compromised by such inhomogeneities (Lindenberg 2011). Here, the yearly mean wind speed shows a sudden increase of about 1.25 m s^{-1} in 1989 when the German Weather Service, the Deutscher Wetterdienst (DWD), relocated the station from an onshore to a coastal place. Also, further improvements in the atmospheric surveillance of the atmosphere through satellites, and an increasing number of buoys and weather stations, lead to an increased detection rate of storm events, which therefore lead to likely false inferences about changes in the past storm climate (Shepherd and Knutson 2007).

In the past decades researchers started to use proxies that are usually based on homogeneous and long pressure observations to avoid these problems. One approach that is feasible for the midlatitudes stems from pressure readings from multiple stations that form triangles to derive geostrophic wind speed statistics over certain areas. This method goes back to Schmidt and von Storch (1993) and has been used in several studies during the years following (e.g., Alexandersson et al. 1998, 2000; Wang et al. 2009). Krueger and von Storch (2011) showed that the triangle proxy describes the variations in the past storm climate reasonably well.

Corresponding author address: Oliver Krueger, Max-Planck-Str. 1, Institute for Coastal Research, Helmholtz-Zentrum Geesthacht, 21502 Geesthacht, Germany.
E-mail: oliver.krueger@hzg.de

Another approach to counteract the problems named is to use pressure readings from single stations directly to derive time series of either annual or seasonal statistics that describe storminess qualitatively. Five kinds of proxies seem commonly used throughout the literature, with slight variations in their individual definitions. These proxies are the number of deep lows (i.e., the number of local pressure observations below a chosen threshold), lower percentiles of pressure, the frequency of absolute pressure tendencies exceeding certain thresholds, as well as high percentiles and mean values of absolute pressure tendencies.

These proxies have been applied to long time series of pressure readings in several regions in the Northern and Southern Hemispheres, often in combination with analyses of geostrophic wind speed statistics. The studies that analyze North Atlantic and European storminess have storminess indices in common that mostly show interdecadal variability, thus rendering any trend non-existent when longer time scales are considered (e.g., Schmith et al. 1998; Jonsson and Hanna 2007; Allan et al. 2009; Bärring and von Storch 2004; Bärring and Fortuniak 2009; Alexander et al. 2005). Most of them also examined to what extent the storminess indices relate to large-scale variability of the atmosphere and analyzed the correlation between the North Atlantic Oscillation (NAO) and past storm activity. Depending on the region examined, they find quite different results. For instance, Scandinavian and central European storminess seems less influenced by the NAO (Bärring and von Storch 2004; Matulla et al. 2008), while storminess over Iceland, the Faroe Islands, and parts of the British Isles is significantly correlated to the NAO (Alexander et al. 2005; Hanna et al. 2008; Allan et al. 2009). In the Southern Hemisphere, studies that use pressure proxies are rare. Alexander and Power (2009), for instance, used twice-daily pressure readings from Australia's Victoria coast to analyze percentiles of pressure tendencies and found that the number of storms along the coast decreased by 40% since the 1850s. Further research appears to be needed to objectively evaluate storminess in the Southern Hemisphere.

The studies that use single-station proxies to evaluate past storminess commonly assume that the variation of the statistics of pressure proxies describes the variation of statistics of ground-level wind speeds. There are some studies that cast doubts on this assumption. Alexandersson et al. (1998) analyzed pressure observation from 21 stations in northwestern Europe and the North Atlantic. They found only low to moderate correlations between time series of geostrophic wind speed percentiles, which can describe storminess qualitatively, and the frequency of high pressure tendencies or the

number of deep lows. The WASA Group (1998) comments on the findings of Alexandersson et al. (1998) that the large-scale low-frequency variability of air pressure shifts local pressure distributions to smaller or larger values without necessarily affecting the storm regime. The authors doubt that counting low pressure occurrences would be useful for assessing storminess. Furthermore, Kaas et al. (1996) suspect that high pressure tendencies, while indicative of strong synoptic disturbances, do not relate to storminess generally, because high pressure tendencies usually do not occur at the same location and time as high wind speeds.

Generally, the pressure proxies are based on synoptic experience and should reflect cyclone activity and storminess changes in the area around a weather station (Bärring and Fortuniak 2009). Until now, the assumption that the variation of the statistics of pressure proxies describes the variation of statistics of ground-level wind speeds has yet to be proven due to a lack of homogeneous wind observations. Thus far, only one study evaluated one of the proxies, albeit through arguable methods: Hanna et al. (2008) assessed the informational content of annual and seasonal mean pressure tendencies. In their study they used observed wind speeds, which were likely inhomogeneous because of weather stations being relocated or changes in the instruments. Furthermore, the authors examined the correlation with mean wind speed time series. They found correlations up to 0.63 and concluded that there would be a general link. However, storm activity relates to strong surface wind speeds. Consequently, we do not know whether mean values of pressure tendencies can describe storminess generally, or whether other proxies can.

For that reason, we aim at a systematic evaluation of the informational value of single-station pressure proxies that are used to describe storm activity. Such an investigation requires long and homogeneous data. Therefore, we use diagnostic 10-m wind and surface air pressure fields from the spectrally nudged and National Centers for Environmental Prediction (NCEP)-driven regional model, REMO (see Feser et al. 2001; Weisse et al. 2009) for the period 1959–2005. These fields belong to the coastDat dataset (available at http://www. coastdat.de from the Helmholtz-Zentrum Geesthacht). The hourly ground-level wind speed and surface air pressure fields cover Europe and the North Atlantic with $0.5° \times 0.5°$ resolution (around 50–60 km). Koch and Feser (2006) compared satellite-retrieved wind data with surface winds simulated in REMO and found that REMO describes wind speeds realistically. Weisse et al. (2005) show that surface wind fields and their statistics are homogeneous and reasonably well simulated over the sea in coastDat. The simulation of (extreme) wind

speeds and their statistics over land highly depends on the physical parameterization scheme. Kunz et al. (2010) note—for a different model version of REMO—that REMO is capable of simulating extreme wind speeds over land. We therefore assume that the wind fields and their statistics are also reasonably well simulated over land.

The remainder of this paper is structured as follows: First, we will introduce the methods that are used, followed by the evaluation of the number of deep lows, lower percentiles of pressure, the frequency of absolute pressure tendencies exceeding certain thresholds, as well as high percentiles and mean values of absolute pressure tendencies for the annual and seasonal time scale, with regard to the thresholds used and other configurations in the proxy definitions. Afterward, we examine whether the proxies can represent large-scale storminess with respect to surface conditions.

2. Evaluation of single-station pressure proxies

a. Tests employed

The assumption that the variation of the statistics of pressure proxies describes the variation of the statistics of ground-level wind speeds implies that the statistics of pressure proxies and high atmospheric wind speeds are positively linearly related. To evaluate this assumption, we first derive annual and seasonal statistics of the proxies. Second, we gauge the derived statistics of proxies against annual (seasonal) 95th and 99th percentile time series of ground-level wind speeds to quantify the relation between pressure-based proxies and storminess. For that reason, we use the correlation as a measure of the informational content of the proxies.

After having derived respective correlations at all of the N grid points within the model domain, the evaluation will be done in two steps. First, we determine the proportions h_+ of positive correlations out of all N correlations. Then, we examine the number h of locally significant correlations.

The first test deals with the null hypothesis

$$H_0^1 : h_+ = 50\% \times N, \tag{1}$$

with the number of positive correlations h_+. Given the null hypothesis H_0^1, the number h_+ is distributed as a binomial distribution $\mathcal{B}(h_+; N; 50\%)$. We reject H_0^1 if

$$\sum_{j \geq h_+} \mathcal{B}(j; N; 50\%) > 95\% \tag{2}$$

at, for instance, the 5% level. The rejection of the null hypothesis will take place when $h_+ > (50\% \times N)$. Then,

the rejection would comply with the acceptance of the alternative hypothesis that, on average, the correlations are positive.

We also test the null hypothesis

$$H_0^2 : h = 1\% \times N, \tag{3}$$

with the number h of correlations, which are found to reject the local null hypothesis of a zero correlation with a risk of 1%. A proportion of $h = 1\%$ is to be expected if there was no link between proxies and wind percentiles. Again, under the null hypothesis H_0^2, the probability of h is given by the binomial distribution $\mathcal{B}(h; N; 1\%)$, and H_0^2 may be rejected with a risk of, for example, 5% if

$$\sum_{j \geq h} \mathcal{B}(j; N; 1\%) > 95\%. \tag{4}$$

Rejection of H_0^2 (because of a too-large h) points to the alternative hypothesis that, on average, the correlations are not locally insignificant.

Both cases of null hypotheses allow an identification of a general positive linear relationship between pressure proxies and storm activity via their rejection. The conditions to reject H_0^1 are easier to meet than those to reject H_0^2. We found that a rejection of H_0^1 is always given when H_0^2 is rejected. On the other hand, a rejection of H_0^2 does not always seem achievable when H_0^1 is rejected. In our case, a rejection of H_0^1 points to a general linear relationship, while a rejection of H_0^2 also indicates a possibly strong general relationship.

The analysis of positive or significant correlations is hampered by the problem of the multiplicity of tests (for details see Livezey and Chen 1983; Storch 1982). We deal with this problem in an ad hoc manner by assuming that the number of independent correlations is $N' = 20$, the numbers h_+ and h are rescaled by N'/N, and N in the binomial distributions is replaced by N'. Then, the product $h' = hN'/N$ (respectively, $h_+ N'/N$) is rounded as the binomial distribution requires integers.

When dealing with low percentiles of pressure readings, which are by design negatively correlated to storminess, we have to reverse the inequalities in (2) and (4) and replace the 95% by 5%.

For every proxy, if necessary, we also assess whether the chosen values in the proxy configurations play an important role for the informational content of the proxies. To do so, we look into significant differences between the median values of the distributions of correlations. The least significant difference, at 0.01 significance, is ± 0.049 for negative–positive differences. We have determined these values from a bootstrapped null distribution of median differences of correlations. Differences
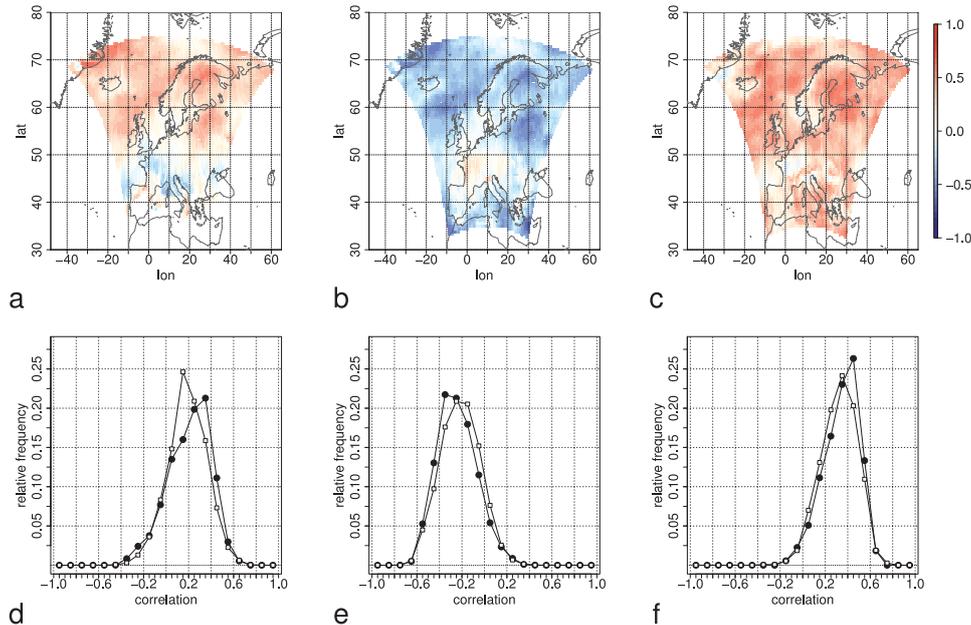
FIG. 1. (top) Spatial distributions of correlations between annual 95th percentiles of surface wind speeds and the annual (a) number of pressure readings below 980 hPa, (b) 1st percentile of pressure readings, and (c) 99th percentiles of absolute pressure tendencies in 24 h. (bottom) The histograms of correlations associated with these proxies in the same order. (d)–(f) The correlation with annual 95th percentiles of surface wind speeds (filled circles) and the correlation with annual 99th percentiles of surface wind speeds (white squares) are shown.

of median correlations are significant at 0.01 significance (which is a rejection of the null hypothesis of a 0 difference), if the differences exceed the given critical values, which are the 0.005 and 0.995 quantiles of the null distribution.

b. Low pressure readings

In this section we concentrate on the proxies based on low pressure readings. We first address the annual and seasonal frequency of pressure readings below a certain threshold. For our evaluation we use 980 hPa as a threshold, which is the value that has been used in most of the studies that deal with past storminess (e.g., Alexandersson et al. 1998; Bärring and von Storch 2004).

Figures 1a,d display the spatial distribution and histograms of correlations between the annual number of pressure readings below 980 hPa and annual 95th and 99th percentiles of surface wind speeds. Table 1 shows the 0.05 quantiles and the median correlation of annual and seasonal correlations. Also shown are the proportion of h_+ and h of positive correlations and rejected local null hypotheses at the 0.01 significance level.

The 0.05 quantiles of the ensembles of correlations are smaller than 0, except for the correlation between the number of pressure readings below 980 hPa and the 95th percentiles of surface wind speeds in spring seasons, which is slightly positive. Median correlations are positive, with values ranging from 0.08 to 0.26, and are

TABLE 1. The 0.05 quantile and median of the distribution of correlations between the number of pressure readings below 980 hPa and 95th and 99th percentiles of surface wind speeds for the annual time scale and the spring [March–May (MAM)], summer [June–August (JJA)], autumn [September–November (SON)], and winter [December–February (DJF)] seasons. Also shown are the proportion h_+ and h of positive correlations and rejected local null hypotheses at the 0.01 significance level. Bold numbers denote 0.01 significance, and italic numbers refer to 0.05 significance.

Ensembles of correlations	0.05 quantile	Median	h_+	h
Annual 95th/99th percentile wind speeds	−0.14/−0.11	0.24/0.19	**85.3%/86.4%**	*10.2%/8.4%*
MAM 95th/99th percentile wind speeds	0.01/−0.03	0.24/0.20	**95.3%/92.6%**	9.9%/3.8%
JJA 95th/99th percentile wind speeds	−0.16/−0.16	0.08/0.08	67.5%/66.5%	2.3%/1.3%
SON 95th/99th percentile wind speeds	−0.03/−0.05	0.17/0.16	**92.1%/89.0%**	0.9%/1.3%
DJF 95th/99th percentile wind speeds	−0.14/−0.11	0.26/0.23	**85.5%/86.0%**	**26.5%/17.7%**

a little higher for the 95th percentiles of surface wind speeds than for the 99th percentiles of surface wind speeds. The differences between median correlations are small; because the values range from 0.16 to 0.26, only the summer seasons have a smaller median correlation of 0.08. We can see in Fig. 1a that positive annual correlations can be found over the sea, Scandinavia, and the Baltic, while other parts of Europe are mostly covered by lower or even negative correlations.

Our analysis reveals, when we look at the proportions h_+ and h, that the sign of correlations is positive in general at the 0.01 significance level, except in the summer season. Only in winter, where the median correlation is highest, is the linear relationship between the number of pressure readings and storminess strong enough to be significant at the 0.01 level. In the winter season, the proportion h of rejected local null hypotheses of a 0 correlation is highest at $h = 26.5\%$. Still, median values of winter correlations remain low. We conclude that the number of pressure readings below 980 hPa is positively linearly linked to storm activity in general on the annual and seasonal time scale, although the informational value is weak.

The low informational value of this proxy partly results from the mean pressure field and its changes over time. The pressure field surrounding a weather station is not necessarily connected to surrounding storminess because high wind speeds can occur independently from low pressure values (WASA Group 1998). Another related reason for the weak informational value is the proxy's sensitivity to counting pressure occurrences below the right threshold. It is very likely that, depending on the threshold, either too few or too many occurrences of pressure readings are counted each year or season. There are, for instance, some regions in Europe that seldom experience pressure readings below 980 hPa, such as Italy. Consequently, the derived time series of low pressure readings might not be connected to storminess at all in such regions. Figure 2 shows the dependence of the median correlation on the chosen threshold. Interestingly, median values only differ slightly, show some variability, and increase with increasing threshold until they peak at 993 (980) hPa for 95th (99th) percentiles of surface wind speeds. The differences among different thresholds are not significant at all (at 0.01 significance). Overall, the distributions of correlations do not change visibly (not shown). However, we noticed that the regional distribution of correlations changes when the threshold increases. While smaller thresholds lead to high correlations over the North Atlantic and small or negative values over Europe, higher thresholds result in high correlations over the Baltic and Scandinavia and lower correlations over the North Atlantic (not
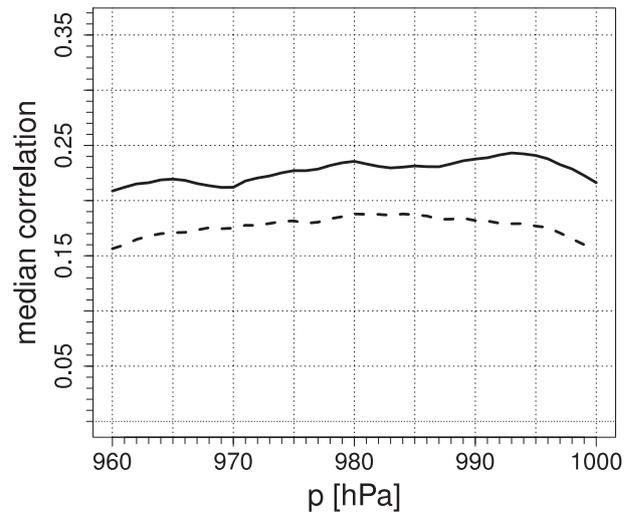
FIG. 2. Dependence of median correlations between the annual number of pressure readings below a certain threshold p and annual 95th (solid line) and 99th percentiles (dashed line) of surface wind speeds depending on the threshold p.

shown). We believe that this behavior comes from the described sensitivity of counting the right number of pressure occurrences.

Similar to the number of low pressure readings, low percentiles of pressure readings are connected to deep lows (Matulla et al. 2012). In contrast to the number of low pressure readings, low percentiles of pressure readings do not suffer from sensitivity to a fixed threshold. In the following we evaluate annual and seasonal first percentiles of pressure. Usually, (very) low pressure readings relate to intense cyclones that bring high wind speeds. Consequently, low pressure percentiles are negatively linked to high wind speeds (Bärring and Fortuniak 2009), meaning that negative correlations between the proxy and high wind speed percentiles indicate informational value. The spatial distribution and histograms of correlations (Figs. 1b,e) indicate that negative correlations cover the North Atlantic, Scandinavia, the Baltic, and the Mediterranean area. Low absolute correlations can be found over central Europe. Median correlations in Table 2 range between −0.20 and −0.28. Winter storminess is best described with median correlations from −0.27 to −0.28. Differences between correlations for 95th and 99th percentiles of surface wind speeds are small, with differences of up to 0.05. From the proportion h_+ we learn that correlations are negative in general. The magnitude of the correlations is in the same order as that of the correlations of low pressure readings. Compared with the number of low pressure readings, median correlations have slightly higher absolute values. Additionally, the proportion h of rejected local

TABLE 2. The 0.95 quantile and median of the distribution of correlations between the annual 1st percentile of pressure readings and annual 95th and 99th percentiles of surface wind speeds for the annual time scale and the spring (MAM), summer (JJA), autumn (SON), and winter (DJF) seasons. Also shown are the proportion h_+ and h of negative correlations and rejected local null hypotheses at the 0.01 significance level. Bold numbers denote 0.01 significance, and italic numbers refer to 0.05 significance.

Ensembles of correlations	0.95 quantile	Median	h_+	h
Annual 95th/99th percentile wind speeds	0.06/0.07	−0.26/−0.21	**91.3%/89.0%**	*14.3%/10.9%*
MAM 95th/99th percentile wind speeds	0.00/0.06	−0.24/−0.20	**94.9%/85.5%**	*14.1%/12.3%*
JJA 95th/99th percentile wind speeds	0.09/0.10	−0.22/−0.20	**86.9%/85.8%**	*13.3%/11.3%*
SON 95th/99th percentile wind speeds	0.04/0.04	−0.22/−0.21	**91.1%/90.1%**	*13.1%/10.4%*
DJF 95th/99th percentile wind speeds	0.09/0.09	−0.28/−0.27	**88.3%/88.9%**	**29.0%/26.0%**

null hypotheses of a 0 correlation is higher because the proportions range from 10.4% to 29.0%. The proportion h is generally significant at the 0.05 level, and is even 0.001 significant for the winter season. The results show that low percentiles of pressure readings are linearly associated with storminess and have higher informational value than the number of low pressure readings, albeit the overall informational value appears weak. The weak informational value follows from the same reason as to why the number of low pressure readings has weak informational content, as given by Bärring and Fortuniak (2009) and Matulla et al. (2012): general changes in the large-scale pressure field can affect the pressure distribution with no obvious changes in storm activity.

c. High absolute pressure tendencies

High local absolute pressure tendencies reflect cyclonic activity and concentrate on high-frequency atmospheric disturbances (Kaas et al. 1996; Schmith et al. 1998). These tendencies denote the absolute pressure difference over a given period Δt. Alexandersson et al. (1998) analyzed the number of absolute pressure tendencies exceeding a threshold of 16 hPa in 24 h, and Bärring and Fortuniak (2009) used 25 hPa in 24 h. Other studies use different thresholds and time periods. A common or established value does not seem to exist throughout the literature. We therefore refrain from evaluating this proxy with a specific value as a threshold in mind. On the other hand, high percentiles of absolute

pressure tendencies only depend on the frequency of available measurements. In the following we will evaluate 99th percentiles of absolute pressure tendencies. Because most of the observed time series were only measured once or twice per day in the long term, we concentrate on pressure tendencies with $\Delta t = 24$ h. We will come back to the choice of thresholds and time intervals later.

Median values of correlations range from 0.27 to 0.37 for all seasons (Table 3). They do not differ much between seasons and between correlations for the 95th and 99th percentiles of wind speed. The spatial pattern of correlations is very similar to the previous proxies. We find high correlations over the North Atlantic, Scandinavia, the Baltic, and the Mediterranean area, and low values over central Europe (Figs. 1c,f). Also, proportions h_+ of positive correlations are high, with values between 92.5% and 97.7%. The proportions h of rejected local null hypotheses vary between 20.4% for summer seasons and 42% for winter seasons. Both h_+ and h are significant at least at the 0.001 significance level, meaning that the proxy is generally linearly linked to storm activity.

Our analyses indicate that the informational value of high percentiles of absolute pressure tendencies is higher than that of the proxies based on low pressure readings. High absolute pressure tendencies partially detect atmospheric disturbances that cause storm activity. The proxy can potentially omit slowly developing disturbances or might detect a disturbance twice when the

TABLE 3. The 0.05 quantile and median of the distribution of correlations between the 99th percentiles of absolute pressure tendencies and 95th and 99th percentiles of surface wind speeds for the annual time scale and the spring (MAM), summer (JJA), autumn (SON), and winter (DJF) seasons. Also shown are the proportion h_+ and h of positive correlations and rejected local null hypotheses at the 0.01 significance level. Bold numbers denote 0.001 significance.

| Ensembles of correlations	0.05 quantile	Median	h_+	h
Annual 95th/99th percentile wind speeds	0.05/0.05	0.37/0.34	**97.2%/97.4%**	**26.3%/21.5%**
MAM 95th/99th percentile wind speeds	0.01/−0.01	0.32/0.29	**95.3%/94.7%**	**33.1%/26.3%**
JJA 95th/99th percentile wind speeds	−0.02/0.01	0.273/0.28	**93.9%/95.7%**	**20.4%/21.8%**
SON 95th/99th percentile wind speeds	−0.05/−0.01	0.30/0.30	**92.5%/94.5%**	**27.9%/29.9%**
DJF 95th/99th percentile wind speeds	0.08/0.07	0.37/0.36	**97.7%/97.7%**	**42.0%/39.4%**
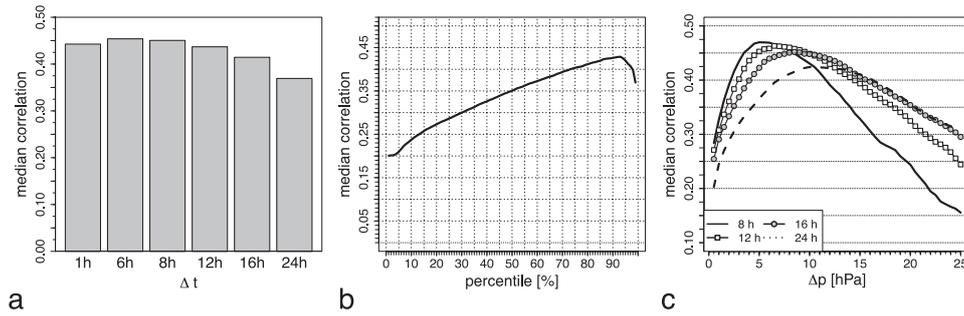
FIG. 3. (a) Dependence of median correlations between annual 95th percentiles of surface wind speeds and the annual 99th percentiles of absolute pressure tendencies on a given time period Δt. (b) The dependence on the percentile of absolute pressure tendencies used to calculate the median correlations with annual 95th percentiles of surface wind speeds. (c) The median correlation with the annual number of absolute pressure tendencies exceeding a certain threshold Δp is shown for different cases of Δt.

pressure is rising (Bärring and Fortuniak 2009). Further, and more importantly, the informational value of pressure tendencies suffers from the fact that high pressure tendencies usually do not occur at the same location and time as high wind speeds (Kaas et al. 1996). We will address this problem in section 3.

As noted earlier, absolute pressure tendencies depend on the choice of Δt. Figure 3a shows the dependence of annual median correlations to the used period Δt. Median correlations are lowest for $\Delta t = 24$ h, with values of 0.37, and highest for $\Delta t = 6$ h, with values of 0.46 for the annual 95th percentiles of surface wind speeds. Differences of median correlations are not significant among different Δt ranging from 1 to 16 h, but are between $\Delta t = 24$ h and the other periods. Also, the informational value gradually decreases with increasing Δt, which becomes understandable when we think of pressure tendencies as a kind of high-pass filters. With smaller values of Δt, absolute pressure differences detect more atmospheric disturbances peaking at $\Delta t = 6$ h. If Δt becomes too small, then atmospheric noise interferes and partially decreases the informational value. We also investigated whether the chosen percentile of absolute pressure tendencies plays a role (Fig. 3b), and found that the highest annual median correlations are obtained for the 93rd

percentiles of absolute pressure tendencies. Higher percentiles than that lead to a small decrease, which means that the higher variability of too-extreme percentiles degrades the informational content.

Another approach used by Hanna et al. (2008) is to calculate annual or seasonal mean values of 24-hourly absolute pressure tendencies. We found that this type of tendency proxy leads to a strong description of storm activity. Annual median correlations are high with values of 0.43 (0.34) for annual 95th (99th) percentiles of surface wind speeds (Table 4). On the seasonal scale, values are similar ranging from 0.34 (0.29) to 0.50 (0.42) for 95th (99th) percentiles of surface wind speeds in the summer and winter season. The spatial distribution is almost equal to that of the other two tendency proxies (not shown), with equal patterns and higher correlations. Also, mean values of 24-hourly absolute pressure tendencies and storminess are generally positively linked, at least at the 0.01 significance level.

In the case of the number of absolute pressure tendencies exceeding a certain threshold, the assessment becomes more complicated. In principle, the number of pressure tendencies exceeding a threshold would have the same informational content as high percentiles of pressure tendencies if the right threshold was chosen.

TABLE 4. The 0.05 quantile and median of the distribution of correlations between the mean value of absolute pressure tendencies and 95th and 99th percentiles of surface wind speeds for the annual time scale and the spring (MAM), summer (JJA), autumn (SON), and winter (DJF) seasons. Also shown are the proportion h_+ and h of positive correlations and rejected local null hypotheses at the 0.01 significance level. Bold numbers denote 0.001 significance, and italic numbers denote 0.01 significance.

Ensembles of correlations	0.05 quantile	Median	h_+	h
Annual 95th/99th percentile wind speeds	0.12/0.05	0.43/0.34	**99.1%/97.8%**	**38.1%**/*19.5%*
MAM 95th/99th percentile wind speeds	0.02/−0.01	0.41/0.32	**96.1%/94.6%**	**51.3%/31.9%**
JJA 95th/99th percentile wind speeds	−0.02/−0.01	0.34/0.29	**94.3%/94.2%**	**31.0%**/*18.4%*
SON 95th/99th percentile wind speeds	0.07/0.03	0.41/0.37	**97.0%/96.2%**	**47.1%/32.1%**
DJF 95th/99th percentile wind speeds	0.16/0.14	0.50/0.42	**99.5%/99.5%**	**67.3%/49.0%**

We calculated median correlations of numbers of pressure tendencies for 8-, 12-, 16-, and 24-hourly values of Δt depending on the threshold Δp in 0.5-hPa increments. First, we see in Fig. 3c that smaller Δt have higher maximum median correlations than greater Δt. Second, we see that for every Δt different optimal thresholds Δp exist. While too-small values of Δp lead to a detection of too much atmospheric noise, and thus decreased informational value, higher values of Δp make the proxy insensitive to atmospheric disturbances. For instance, the median correlation of the number of pressure tendencies with $\Delta t = 8$ h peaks at $\Delta p = 5.5$ hPa, with a correlation of 0.47, and decreases thereafter steeply. Further, median correlations for $\Delta t = 24$ h are highest at a value of 0.42 when the threshold Δp is 10.0 hPa. The fact that thresholds, which are smaller than those used throughout the literature, lead to higher correlations emphasizes the point given by Kaas et al. (1996) that high pressure tendencies do not occur simultaneously with strong synoptic disturbances. In that case, smaller thresholds lead to an improvement in the detection of atmospheric disturbances that pass by in some distance. However, our sensitivity analysis reveals that it might be possible to optimize the description of past storminess for a given period Δt, which the frequency of measurements often determines, when the right threshold Δp is selected.

We have obtained all of the results through simulated winds in REMO. Because the statistics of atmospheric wind speeds are reasonably well simulated over sea (Feser et al. 2011), we expect that our obtained results are applicable in the real atmosphere, though we cannot estimate the real informational value of the proxies because of a lack of homogeneous wind speed observations.

3. Can single-station proxies represent large-scale storm activity?

Wind speed and storm activity primarily depend on an atmospheric pressure gradient. Such a pressure gradient is caused by atmospheric disturbances that pressure proxies seek to detect. However, as noted, it is very likely that strong atmospheric disturbances and winds occur remotely from the actual place where pressure measurements are taken. As a result, we would find a weakened link between storminess and pressure proxies at a certain place. On the contrary, we believe that the described characteristics can be used to make inferences about storminess in a larger area surrounding a station.

To examine such a dependence, we look into median correlations between two proxies and annual 95th and 99th percentiles of area-maximum surface wind speeds within a square of variable size surrounding the grid

point from which the pressure has been taken to derive the proxies. The length of the sides of these squares depends on the geographical latitude. The squares are thus deformed to spherical rectangles. We have selected 1013 grid points from the model domain randomly to conduct our analyses. We concentrate on two proxies only, namely, the annual 1st percentile of pressure and the 99th percentile of absolute pressure tendencies to avoid further complications resulting from threshold dependencies. In our approach, which enhances the analyses of Kaas et al. (1996), the length of sides varies from 3 to 21 grid points, with a minimum length of about 120 km and a maximum length of about 1200 km. The average size of sides denotes the scale, on which the pressure proxies would represent storm activity, which we label as scale. The scale is divided into four classes: extra small, small, medium, and large. Large scales are scales of greater than 800 km, which mark the transition from the mesoscale to synoptic scales. The extra small class reaches up to 300 km, which includes the characteristic horizontal range of cold fronts that stretch from 80 to 300 km (Carlson 1991). Cold fronts that bring a transition from warmer to colder air masses are typical atmospheric disturbances in the extratropics. They are often accompanied by strong winds and falling or low pressure. We divided the scales in between the extra small and large class into two classes to achieve almost balanced group sizes. The small class denotes scales that are either smaller than or equal to 550 km, while the medium scale is smaller than or equal to 800 km, but greater than 550 km. In addition, we classified correlations as either land or sea to assess the informational content of proxies regarding surface conditions. The surface condition within a rectangle is classified as land for a land fraction of greater than 0.5 and as sea for a land fraction of equal to or smaller than 0.5. The results are presented in Fig. 4.

Consider first the median correlations between the annual 99th percentile of absolute pressure tendencies and the 95th percentiles of area-maximum surface wind speeds (Fig. 4a). The informational content over the combined land and sea surfaces remains almost constant over small and medium scales, with correlations slightly rising from 0.39 to about 0.42, and then decreasing a little to 0.39. Although the correlations do not vary much when increasing scales are regarded, it seems that absolute pressure tendencies are better at representing storminess within a greater area surrounding one station than at one particular point. Over sea, median correlations remain at about 0.42–0.45, with the highest correlation of 0.46 for medium scales. Over land, the correlations rise from 0.35 to about 0.38 at medium scales and decrease to 0.36 for large scales. Overall, the
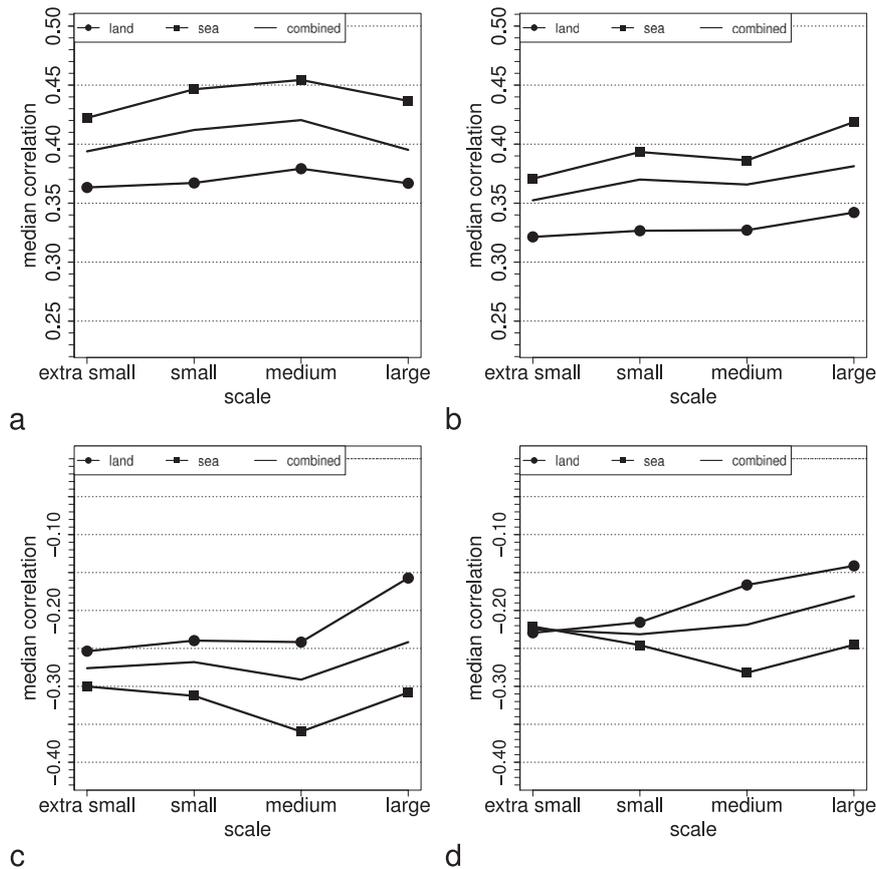
FIG. 4. Median annual group correlations of (a),(b) 99th percentiles of absolute pressure tendencies in 24 h and (c),(d) 1st percentiles of pressure with (left) 95th and (right) 99th percentiles of area-maximum surface wind speeds within a square of variable size surrounding grid points where the proxies have been calculated. We determined these squares by grid points. For that reason, the length of sides differs within a square because of different geographical latitudes. Shown are the median group correlations vs the average size of sides that represent the distance, on which pressure proxies might describe storm activity, for land, sea, and combined land–sea rectangles.

differences between land and sea surfaces are significant and between 0.05 and 0.1, suggesting that absolute pressure tendencies are not overly affected by surface properties. The higher informational value of the pressure tendencies probably compensates for the deterioration resulting from surface conditions.

Consider now the median correlations between the annual 1st percentile of pressure and 95th percentiles of area-maximum surface wind speeds. Note that negative correlations indicate informative value. Independent from surface conditions (solid line in Fig. 4c), the informational content increases between extra small and medium scales as the median correlation decreases from −0.27 to −0.29. For large scales, the correlation increases to −0.24. When compared with the annual median correlation at the same place (−0.26 from Table 2), we see that within the small and medium scales the informational

content is somewhat superior, although differences are not significant (at the 0.01 level). A similar picture can be seen when we regard the influence of land and sea surface conditions. For sea surfaces, the informational content rises more drastically within the small to medium scales with correlations from −0.30 to −0.36 and decreases afterward to a correlation of −0.30. For land surfaces, the correlations increase slightly from −0.25 to −0.24 within small and medium scales, and steeply for large scales to −0.16. The differences in median correlations between land and sea surfaces grow from 0.05 to 0.20. Turbulent effects and ageostrophic dynamics over land that alter surface winds in the planetary boundary layer are responsible for the deterioration of the informational content over land. Over sea the frictional influence from the surface diminishes, resulting in a better description of storminess

through low pressure. However, the informational value of low pressure readings remains low.

When we look at the correlations with more extreme percentiles (namely, the 99th) of area-maximum surface wind speeds (Figs. 4b,d), we notice some differences and similarities. First, the differences between land and sea surfaces range between 0.05 and 0.08 for the 99th percentile of absolute pressure tendencies. For the first percentile of pressure, on the contrary, the differences vanish for extra small scales and increase by 0.1 to large scales. The informational content over sea increases for both proxies within small and medium scales, and either decreases afterward (1st percentile of pressure) or remains almost constant (99th percentile of absolute pressure tendencies). The informational content decreases over land steadily with increasing scale for the first percentile of pressure. For the 99th percentile of absolute pressure tendencies it does not change significantly. Second, correlations are about 0.05 smaller than that of correlations with 95th percentiles of area-maximum surface wind speeds. Overall absolute correlations of the first percentile of pressure decrease from 0.23 to 0.13. At the same, the overall correlations of the 99th percentile of absolute pressure tendencies grow slightly, increasing from 0.35 to 0.38 within the scales. The higher variability of the 99th percentile of area-maximum surface wind speeds obviously makes the description of more extreme storm activity through pressure proxies difficult, especially at the extra small scales.

Generally speaking, we see that the 99th percentile of absolute pressure tendencies performs better in describing storm activity than the 1st percentile of pressure, in particular, over larger scales. Furthermore, we looked into the median correlations of high percentiles of absolute pressure tendencies with $\Delta t = 8$ h, because $\Delta t = 8$ h results in one of the highest informational contents (Fig. 3). Our analysis reveals that the behavior is very similar to the case of $\Delta t = 24$ h. The correlations with 95th percentiles of area-maximum surface wind speeds remain at about 0.5 for sea surfaces and 0.45 for land surfaces, and slightly decrease to 0.42 on large scales for land surfaces. The differences between land and sea surfaces grow from 0.05 to 0.09 throughout the scales. The correlation with 99th percentiles of area-maximum surface wind speeds for combined surface properties is about 0.42 for all scales. Over sea, the correlation increases from 0.42 to 0.45 from extra small to small scales and remains at that value. Over land, the correlation decreases from 0.42 to 0.35 from extra small to large scales. The differences between land and sea surfaces vanish for extra small scales and increase to about 0.1 throughout the scales. The differences are little over

extra small scales because of the higher informational content that results from a smaller Δt.

The presented results also depend on the classification criteria for land and sea surfaces. We have used a land fraction of 0.5 as the threshold to distinguish between land and sea surfaces, which include mixed surface conditions. When making use of stricter thresholds we would expect higher absolute correlations over sea surfaces, because the influence of land surfaces would become weaker. Absolute correlations that follow from stricter thresholds to classify land and sea conditions (e.g., a land fraction smaller than 0.2 for sea surfaces and larger than 0.8 for land surfaces) are indeed different to the aforementioned results (not shown). Resulting correlations over land and sea surfaces behave almost the same qualitatively, but the differences between land and sea surfaces become more distinct. Further, the magnitude of the median correlations rises more drastically with increasing scales. Correlations of high pressure tendencies increase to 0.53 (0.47) when compared with 95th (99th) percentiles of area-maximum wind speed over sea at large scales. At the same, the correlation does not increase much over land surfaces. We also see an increased magnitude in the correlations of low pressure percentiles, in particular, over sea surfaces (up to −0.48).

Note that described effects strongly depend on the parameterization in the used limited area model. Atmospheric stability and frictional effects of vegetation cover and topography affect the near-surface winds, but because of the subgrid-scale processes involved, these effects are only parameterized on the subgrid scale in models. The influence of the details of these parameterizations on obtained median correlations is unknown and needs to be examined elsewhere. However, within the model the physics are consistent, making our results reliable. We can only speculate whether an advanced parameterization or a finer spatial resolution would either improve modeled winds or alter our results significantly.

4. Concluding remarks

This study systematically evaluates several single-station pressure-based proxies that have been and probably will be used to assess past and recent storm activity in the midlatitudes. We gauged the proxies against 95th and 99th percentiles of ground-level wind speeds and calculated correlations, which we use as a measure of informational value. Our results from examining the informational content of five different proxies indicate that the proxies are linked to storm activity in general. For the number of low pressure readings and low percentiles

of pressure we found only weak informational value (absolute correlations of about 0.26), while proxies that are based on absolute pressure tendencies have higher informational value (up to a correlation of about 0.5 for mean tendencies). We also found that the correlations are systematically lower for the 99th percentiles of ground-level wind speeds because of the higher variability of extreme wind speeds. If, however, the informational value of the statistics of geostrophic wind speeds (Krueger and von Storch 2011) is taken as a standard, we see that even the statistics of absolute pressure tendencies have weaker informational value. Wind speeds in the midlatitudes directly relate to a pressure gradient that determines geostrophic wind speeds. Pressure tendencies, on the contrary, detect atmospheric disturbances and relate to storminess indirectly.

The tendency proxy that counts threshold exceedances is very sensitive to the threshold chosen, while the number of low pressure readings is insensitive toward changing the threshold value. When statistics of absolute pressure tendencies are considered, we find higher informational value when not too extreme percentiles or mean values are used.

Absolute pressure tendencies also have the potential of describing storminess for a larger area surrounding a weather station, which we have seen in a higher correlation on larger scales. Over sea, the proxies generally show higher informational value than over land. The informational value of low pressure readings, on the other hand, does improve considerably on increasing scales. Further, when comparing the first percentile of pressure with more extreme wind speeds within small scales, the differences even vanish between land and sea surfaces.

We found our results by using simulated air pressure and ground-level wind speed in REMO. We expect that our findings are as relevant in the real atmosphere as they are in the simulation.

REFERENCES

Alexander, L., and S. Power, 2009: Shorter contribution: Severe storms inferred from 150 years of sub-daily pressure observations along Victoria's shipwreck coast. *Aust. Meteor. Oceanogr. J.,* **58,** 129–133.

——, S. Tett, and T. Jonsson, 2005: Recent observed changes in severe storms over the United Kingdom and Iceland. *Geophys. Res. Lett.,* **32,** L13704, doi:10.1029/2005GL022371.

Alexandersson, H., T. Schmith, K. Iden, and H. Tuomenvirta, 1998: Long-term variations of the storm climate over NW Europe. *Global Atmos. Ocean Syst.,* **6,** 97–120.

——, H. Tuomenvirta, T. Schmith, and K. Iden, 2000: Trends of storms in NW Europe derived from an updated pressure data set. *Climate Res.,* **14,** 71–73.

Allan, R., S. Tett, and L. Alexander, 2009: Fluctuations in autumn–winter severe storms over the British Isles: 1920 to present. *Int. J. Climatol.,* **29,** 357–371.

Bärring, L., and H. von Storch, 2004: Scandinavian storminess since about 1800. *Geophys. Res. Lett.,* **31,** L20202, doi:10.1029/2004GL020441.

——, and K. Fortuniak, 2009: Multi-indices analysis of southern Scandinavian storminess 1780–2005 and links to interdecadal variations in the NW Europe-North Sea region. *Int. J. Climatol.,* **29,** 373–384.

Carlson, T. N., 1991: *Midlatitude Weather Systems*. HarperCollins Academic, 507 pp.

Feser, F., R. Weisse, and H. von Storch, 2001: Multi-decadal atmospheric modeling for Europe yields multi-purpose data. *Eos, Trans. Amer. Geophys. Union,* **82,** 305.

——, B. Rockel, H. von Storch, J. Winterfeldt, and M. Zahn, 2011: Regional climate models add value to global model data: A review and selected examples. *Bull. Amer. Meteor. Soc.,* **92,** 1181–1192.

Hanna, E., J. Cappelen, R. Allan, T. Jónsson, F. Le Blancq, T. Lillington, and K. Hickey, 2008: New insights into north European and North Atlantic surface pressure variability, storminess, and related climatic change since 1830. *J. Climate,* **21,** 6739–6766.

Jonsson, T., and E. Hanna, 2007: A new day-to-day pressure variability index as a proxy of Icelandic storminess and complement to the North Atlantic oscillation index 1823–2005. *Meteor. Z.,* **16,** 25–36.

Kaas, E., T. Li, and T. Schmith, 1996: Statistical hindcast of wind climatology in the North Atlantic and north-western European region. *Climate Res.,* **7,** 97–110.

Koch, W., and F. Feser, 2006: Relationship between SAR-derived wind vectors and wind at 10-m height represented by a mesoscale model. *Mon. Wea. Rev.,* **134,** 1505–1517.

Krueger, O., and H. von Storch, 2011: Evaluation of an air pressure–based proxy for storm activity. *J. Climate,* **24,** 2612–2619.

Kunz, M., S. Mohr, M. Rauthe, R. Lux, and C. Kottmeier, 2010: Assessment of extreme wind speeds from regional climate models–Part 1: Estimation of return values and their evaluation. *Nat. Hazards Earth Syst. Sci.,* **10,** 907–922.

Lindenberg, J., 2011: A verification study and trend analysis of simulated boundary layer wind fields over Europe. Ph.D. dissertation, University of Hamburg, 116 pp.

Livezey, R., and W. Chen, 1983: Statistical field significance and its determination by Monte Carlo techniques. *Mon. Wea. Rev.,* **111,** 46–59.

Matulla, C., W. Schöner, H. Alexandersson, H. von Storch, and X. Wang, 2008: European storminess: Late nineteenth century to present. *Climate Dyn.,* **31,** 125–130.

——, M. Hofstätter, I. Auer, R. Böhm, M. Maugeri, H. von Storch, and O. Krueger, 2012: Storminess in northern Italy and the Adriatic Sea reaching back to 1760. *Phys. Chem. Earth,* **40–41,** 80–85, doi:10.1016/j.pce.2011.04.010.

Schmidt, H., and H. von Storch, 1993: German Bight storms analysed. *Nature,* **365,** 791–791.

Schmith, T., E. Kaas, and T. Li, 1998: Northeast Atlantic winter storminess 1875–1995 re-analysed. *Climate Dyn.,* **14,** 529–536.

Shepherd, J., and T. Knutson, 2007: The current debate on the linkage between global warming and hurricanes. *Geogr. Compass,* **1,** 1–24, doi:10.1111/j.1749-8198.2006.00002.x.

Storch, H., 1982: A remark on Chervin-Schneider's algorithm to test significance of climate experiments with GCM's. *J. Atmos. Sci.,* **39,** 187–189.

Trenberth, K., and Coauthors, 2007: Observations: Surface and atmospheric climate change. *Climate Change 2007: The Physical Science Basis,* S. Solomon et al., Eds., Cambridge University Press, 312–315.

Wang, X., F. Zwiers, V. Swail, and Y. Feng, 2009: Trends and variability of storminess in the Northeast Atlantic region, 1874–2007. *Climate Dyn.,* **33,** 1179–1195.

WASA Group, 1998: Changing waves and storms in the Northeast Atlantic? *Bull. Amer. Meteor. Soc.,* **79,** 741–760.

Weisse, R., H. von Storch, and F. Feser, 2005: Northeast Atlantic and North Sea storminess as simulated by a regional climate model 1958–2001 and comparison with observations. *J. Climate,* **18,** 465–479.

——, and Coauthors, 2009: Regional meteorological–marine reanalyses and climate change projections: Results for Northern Europe and potentials for coastal and offshore applications. *Bull. Amer. Meteor. Soc.,* **90,** 849–860.

Inconsistencies between Long-Term Trends in Storminess Derived from the 20CR Reanalysis and Observations

OLIVER KRUEGER, FREDERIK SCHENK, FRAUKE FESER, AND RALF WEISSE

Institute for Coastal Research, Helmholtz-Zentrum Geesthacht, Geesthacht, Germany

ABSTRACT

Global atmospheric reanalyses have become a common tool for both validation of climate models and diagnostic studies, such as assessing climate variability and long-term trends. Presently, the Twentieth Century Reanalysis (20CR), which assimilates only surface pressure reports, sea ice, and sea surface temperature distributions, represents the longest global reanalysis dataset available covering the period from 1871 to the present. Currently the 20CR dataset is extensively used for the assessment of climate variability and trends. Here, the authors compare the variability and long-term trends in northeast Atlantic storminess derived from 20CR and from observations. A well-established storm index derived from pressure observations over a relatively densely monitored marine area is used. It is found that both variability and long-term trends derived from 20CR and from observations are inconsistent. In particular, both time series show opposing trends during the first half of the twentieth century: both storm indices share a similar behavior only for the more recent periods. While the variability and long-term trend derived from the observations are supported by a number of independent data and analyses, the behavior shown by 20CR is quite different, indicating substantial inhomogeneities in the reanalysis, most likely caused by the increasing number of observations assimilated into 20CR over time. The latter makes 20CR likely unsuitable for the identification of trends in storminess in the earlier part of the record, at least over the northeast Atlantic. The results imply and reconfirm previous findings that care is needed in general when global reanalyses are used to assess long-term changes.

1. Introduction

Global atmospheric reanalyses have become a common tool for climate model validations and diagnostic studies such as assessing climate variability and long-term trends. In operational weather analyses, state-of-the-art numerical weather prediction models in combination with modern data assimilation schemes are used to project the state of the atmosphere as described by a finite set of imperfect, irregularly distributed observations onto a regular grid (Glickman 2000). These analyses are useful products for numerical weather forecasts, but their use in climate change research remains limited because changes in the analysis system (the model or the data assimilation scheme) or changes in the observational network used may introduce inhomogeneities, which may cause spurious trends. To reduce inhomogeneities, a

number of global reanalysis efforts (e.g., Uppala et al. 2005; Kalnay et al. 1996; Onogi et al. 2007) have been developed, all using frozen state-of-the-art data assimilation systems and numerical models. In this way, inhomogeneities in global reanalyses are greatly reduced, although changes in the (assimilated) observational network data may still have substantial impacts. For example, Bengtsson et al. (2004) showed that a remarkable jump in the annually averaged total kinetic energy occurred in the 40-yr European Centre for Medium-Range Weather Forecasts Re-Analysis (ERA-40) (Uppala et al. 2005) at the time when satellite data were introduced into the reanalysis, which lead to a significant upward trend in the total kinetic energy. This trend was largely reduced in a sensitivity experiment that simulated the situation before the advent of satellite data. Kistler et al. (2001) computed annually averaged anomaly correlations between 5-day forecasts of 500-hPa heights, which were initiated from the National Centers for Environmental Prediction–National Center for Atmospheric Research (NCEP–NCAR) reanalysis and the reanalysis itself at the time of the forecast. For the Northern

Hemisphere they found that forecast skill was steadily increasing with time for the first 10 years or so of the reanalysis. These results indicate that during that time the quality (or the degree of realism) of the reanalysis has steadily improved owing to more and better observations and that the first 10 yr should be discarded when assessing long-term changes. Moreover, they showed that the reanalysis is much better over the Northern than over the Southern Hemisphere where much fewer observations are available, a result that is found and confirmed also from reanalyses products (e.g., Bromwich et al. 2007).

So far, most reanalyses available cover periods of up to several decades mostly for the second half of the twentieth century. While the datasets in recent decades might be less affected by inhomogeneities, the records are too short to fully assess natural climate variability and long-term changes. Therefore, the Twentieth Century Reanalysis project has been set up to produce a comprehensive global atmosphere dataset covering the period from 1871 onward (Compo et al. 2011). By assimilating only surface pressure observations with sea ice and sea surface temperature anomalies as boundary conditions, it was anticipated that inhomogeneities are largely reduced and, furthermore, that the dataset will become a valuable resource for both climate model validations and diagnostic studies (Compo et al. 2011). Some surprising results, such as noticeable differences of long-term trends in zonally averaged precipitation minus evaporation derived from the Twentieth Century Reanalysis (20CR) and from climate model simulations of the twentieth century, are already noted by Compo et al. (2011). Ferguson and Villarini (2012) recently found inhomogeneities in 20CR air temperature and precipitation that led to their suggestion to restrict climate trend applications over the central United States to the second half-century of the 20CR records.

More recently some papers have been published concentrating on assessing long-term trends in storm activity over Europe using 20CR. Brönnimann et al. (2012) used 20CR to assess trends in storm activity from 1871 onward by using modeled wind speeds at every grid point of 20CR in the Northern Hemisphere. In different case studies they find consistency with observations (e.g., the storm Kyrill). They also find good agreement with long-term storminess at Zurich (observed and modeled) where long observations of wind speed are available.

Donat et al. (2011) used 20CR to provide an analysis of storminess throughout the period 1871–2008. Through the assessment of a gale index derived from air pressure differences and upper percentiles of daily maximum wind speeds, they concluded that 20CR suggests a long upward trend in European storminess since 1871. They mention the possibility that 20CR is likely to suffer from inhomogeneities due to changing station density and quality of early observations. However, they conclude that the observational density over Europe is relatively high throughout the investigated period and suggest that identified trends may (at least partially) be a consequence of increasing greenhouse gas concentrations during the past. Their result is in sharp contrast to a large number of studies focusing on long-term storminess trends for western Europe and the North Atlantic (e.g., Alexandersson et al. 2000; Bärring and von Storch 2004; Matulla et al. 2008; Wang et al. 2009), which found decreasing storminess until the 1960s, an increase until the mid-1990s, and a decline afterward.

In this paper we focus on the extent to which long-term trends in storm activity over Europe and the northeast Atlantic may be derived from 20CR. Instead of relying on wind speed measurements themselves, which frequently suffer from inhomogeneities such as changes in measurement techniques, relocation of stations, or changes in the surrounding of stations (e.g., Wan et al. 2010; Lindenberg et al. 2012), we use a well-established proxy for storm activity based on geostrophic wind speeds derived from surface pressure data. The index was originally proposed by Schmidt and von Storch (1993) and later on extensively used by other authors (e.g., Alexandersson et al. 2000; Bärring and von Storch 2004; Matulla et al. 2008; Wang et al. 2009). Krueger and von Storch (2011) showed that the informational content of such proxies is high enough to describe past storminess. Updates of such indices are provided in the Intergovernmental Panel on Climate Change (IPCC) Fourth Assessment Report to describe long-term changes and variability of storm activity (Fig. 3.41 in Trenberth et al. 2007). Moreover, marine surface pressure measurements are less likely to be affected by inhomogeneities as marine surface pressure represents (compared to near-surface wind speeds) a relatively large-scale variable that is less affected by changes in instrumentation,[1] small relocations of stations, or changes in the surrounding stations. We also concentrate on an area known to have a relatively high station density throughout the period for which 20CR was performed (Donat et al. 2011) in order to provide a conservative estimate.

The remainder of this paper is structured as follows. In the next section, we concentrate on the comparison of storminess trends in 20CR and observations. We first introduce the data and method needed in our analysis and present the results afterward. In the third section, we assess changes in the number of stations assimilated

---

[1] Pressure is measured over centuries using mercury barometers.

into 20CR, followed by the last section in which we discuss our results and conclude.

2. Comparison of storminess trends in 20CR and observations

a. Data and methods

Upper percentiles of geostrophic wind speeds are derived from triangles of mean sea level pressure (MSLP) time series. The exact details of this method are given in Schmith (1995) and Wang et al. (2009). Only three different time series of pressure readings are needed to describe storminess over the area of one triangle independently from measurements within the triangle. At each location ($x = R_e\lambda\cos\phi$, $y = R_e\phi$) (where R_e denotes the earth's radius, λ the longitude, and ϕ the latitude), the pressure p is described as

$$p = ax + by + c. \qquad (1)$$

The coefficients a, b, and c are unique for each triangle and can be derived through solving the following set of equations:

$$\begin{aligned} p_1 &= ax_1 + by_1 + c \\ p_2 &= ax_2 + by_2 + c \\ p_3 &= ax_3 + by_3 + c. \end{aligned} \qquad (2)$$

The geostrophic wind speed is then calculated as

$$U_{\text{geo}} = (u_g^2 + v_g^2)^{1/2} \qquad (3)$$

with

$$u_g = -\frac{1}{\rho f}\frac{\partial p}{\partial y} = -\frac{b}{\rho f}; \quad v_g = \frac{1}{\rho f}\frac{\partial p}{\partial x} = \frac{a}{\rho f}, \qquad (4)$$

where ρ is the density of air (set at 1.25 kg m^{-3}) and f the Coriolis parameter. The coefficients a and b denote the zonal and meridional pressure gradients. Note that f is usually the average of the Coriolis parameter at each measurement site. After having derived U_{geo} at each time step, time series of geostrophic wind speed statistics can be obtained.

The MSLP observations used in our study are available from Cappelen et al. (2010). The pressure observations are also available from the International Surface Pressure Database (at http://reanalyses.org/observations/international-surface-pressure-databank), whose data have been assimilated into 20CR (Compo et al. 2011). Presumably, storm activity based on observations and on 20CR should be very similar.
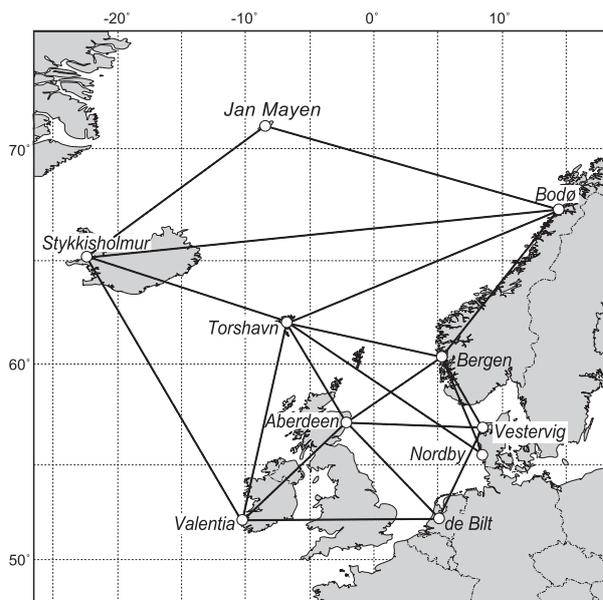

FIG. 1. Pressure observations from various stations have been used to derive geostrophic wind speed time series over 10 triangles over northeast Atlantic and European regions. A detailed description of the data is given in Alexandersson et al. (1998, 2000) and Cappelen et al. (2010).

We derive the standardized time series of annual 95th and 99th percentiles of geostrophic wind speeds over 10 triangles of mean sea level pressure from observations and 20CR in the North Atlantic from 1881 onward. The time series are standardized by subtracting their mean values and dividing by their standard deviations as in Alexandersson et al. (1998, 2000). The standardization ensures that each time series is in the same range. We only regard annual percentiles to prevent the possible danger of alias artifacts in the time series (see Madden and Jones 2001). Afterward, these 10 time series are averaged to obtain a robust estimate of storminess on a large scale. The coordinates of the triangle corners are given by Alexandersson et al. (1998, 2000) and are illustrated in Fig. 1. In 20CR, we use the grid boxes nearest to the station coordinates (see Fig. 1 and Table 1). Note that, in the case of the Danish stations, the two stations lie within one 20CR grid point. Although the MSLP values from 20CR grid points are not identical to station measurements, resulting differences are systematic throughout the gradient calculation. Therefore, the statistics of the geostrophic wind speeds will not be affected greatly by this issue. Further, the MSLP is a relatively large-scale variable. By employing our analysis over sea surfaces mainly, we minimize the influence of land surfaces and avoid land-use change (or changes in surface roughness). These aspects would disturb the geostrophic wind approximation and thus its representativeness of surface

TABLE 1. WMO number (or for Denmark a national climate number), country, name, and coordinates of the stations used. The numbers in parentheses denote the coordinates of the nearest 20CR grid box.

Number	Country	Name	Lat	Lon
01001	Norway	Jan Mayen	70.93°N (70°N)	8.67°W (8°W)
01152	Norway	Bodø	67.27°N (68°N)	14.43°E (14°E)
01316	Norway	Bergen	60.38°N (60°N)	5.33°E (6°E)
03091	Great Britain	Aberdeen	57.2°N (58°N)	2.2°W (2°W)
03953	Ireland	Valentia	51.93°N (52°N)	10.25°W (10°W)
04013	Iceland	Stykkisholmur	65.08°N (66°N)	22.73°W (22°W)
06011	Faroe Islands	Torshavn	62.02°N (62°N)	6.77°W (6°W)
06260	Netherlands	de Bilt	52.1°N (52°N)	5.18°E (6°E)
21100	Denmark	Vestervig	56.73°N (56°N)	8.27°E (8°E)
25140	Denmark	Nordby	55.47°N (56°N)	8.48°E (8°E)

storminess (Krueger and von Storch 2011). However, the geostrophic wind itself and its statistics are independent from such aspects.

We repeat the calculations for each of the 56 ensemble members of 20CR and derive an ensemble mean of the storminess time series in 20CR as suggested by Compo et al. (2011). In the following, we will concentrate on the standardized annual 95th percentiles of geostrophic wind speeds only as both standardized time series derived from annual 95th and 99th percentiles agree almost completely with each other.

We focus our discussion on Gaussian-filtered time series (with $\sigma = 3$), which leaves the long-term trends in the time series without the year-to-year variability. We provide the Gaussian-filtered ensemble mean of the 56 percentile time series, the associated (Gaussian-filtered ensemble) spread (black line and gray shades in Fig. 2), and the Gaussian-filtered percentile time series derived from observations (blue line in Fig. 2). Along with averaging the time series of the 10 triangles and only regarding annual percentiles, the Gaussian filter will help to overcome potential problems in comparing the time series that may arise from the different temporal resolution of 20CR (6-hourly) and observations (3-hourly, and later 1-hourly). Note that we have taken the missing years in the observations (see Table 2) into account by setting these years to missing values at the respective locations in the 20CR data. Our analysis of storminess therefore starts in the year 1881. Even so, the same observations have been very likely assimilated into 20CR. Considering all these measures taken, our employed analysis provides a robust estimate of storm activity on a large scale.

b. Comparison of storminess and statistical significance

Storminess derived from 20CR through geostrophic wind speeds over the northeast Atlantic resembles the time series shown in Donat et al. (2011); in particular, an upward trend over the whole period is inferred. The time series increases until the 1990s and then decreases. Moreover, some decadal variability is imposed on the time series, which appears to be weak.

However, when compared with the 95th percentiles of geostrophic wind from observations after Alexandersson et al. (2000) (blue line in Fig. 2), we obtain completely different results. Except from a decline in the 1880s, a trend over the entire analysis period derived from observations is not visible. Decadal-scale variability dominates the observation-based time series. There is only one similarity: The time series seem to be in phase after
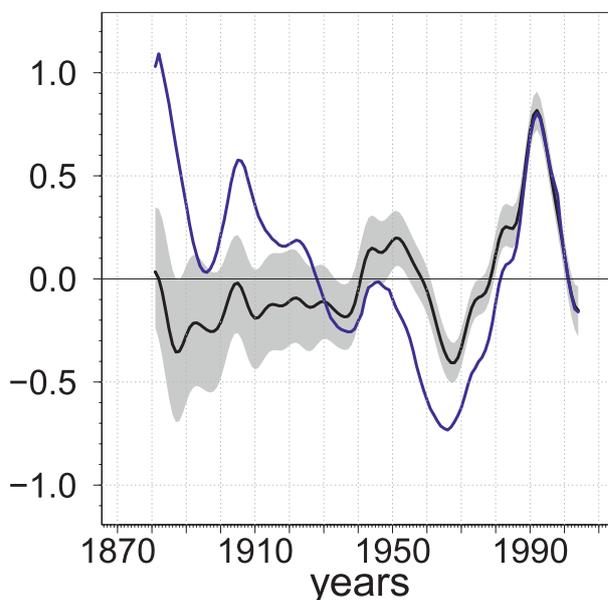

FIG. 2. Standardized time series of annual 95th percentiles of geostrophic wind speeds over 10 triangles in the North Atlantic, which have been averaged and low-pass filtered thereafter. The black line denotes the ensemble mean of these time series in 20CR, along with the complete associated ensemble spread, which is represented by the minimum and maximum values of the ensemble. The blue line is reconstructed after Alexandersson et al. (2000) for the period 1881–2004.

TABLE 2. Triangles and time periods used to construct mean values within the northeast Atlantic.

Triangle	Period
Torshavn–Stykkisholmur–Bodø	1900–2004
Bergen–Torshavn–Aberdeen	1881–2004
Torshavn–Bodø–Bergen	1900–2004
Aberdeen–Valentia–Torshavn	1892–2004
Bergen–Vestervig–Aberdeen	1881–2004
Aberdeen–Valentia–de Bilt	1902–2004
Aberdeen–Vestervig–de Bilt	1902–2004
Valentia–Stykkisholmur–Torshavn	1892–2004
Jan Mayen–Stykkisholmur–Bodø	1922–2004
Torshavn–Nordby–Bergen	1881–2004

1940 and share a correlation of 0.95. Before 1940 the correlation is 0.11. Either time series share the upward trend after the 1960s and the following decreasing trend starting in the early 1990s. During the same period the differences almost vanish. In contrast to our 20CR-based time series, the upward trend in storminess from observations after 1960 is rather small (relative to the whole time series itself).

Formally, our findings are confirmed by bootstrap hypothesis testing of differences in low-pass filtered mean values, which allows us to also consider uncertainties in the observations. First, we derive an ensemble of similar observation-based time series of mean sea level pressure through sampling measurement errors. In this first step, we assume normally distributed measurement errors in the pressure observations with a mean of 0 hPa and a standard deviation of 1 hPa. Note that this value is rather conservative and high as pressure observations are usually provided with 0.1-hPa accuracy. Such a high value of 1 hPa, nevertheless, ensures that larger uncertainties in measurements in the early years are well accounted for. These random errors are repeatedly added to the observed mean sea level pressure, from which annual 95th percentiles of geostrophic wind speeds are then calculated (as written above). The created ensemble, in our case, consists of 7400 storminess time series, whose ensemble mean is low-pass filtered (see above) and compared to the low-pass filtered ensemble mean of 20CR storminess in the next step. Second, under the null hypothesis of no differences in low-pass filtered mean values, we bootstrapped a null distribution to derive upper and lower critical values of differences. At the 0.01 significance level, these values are about ±0.14. Last, we calculated the differences in low-pass filtered mean values (i.e., between the black and blue line) at each time step of the overlapping time period 1881–2004. There are only two periods when differences are in between the calculated critical values and thus fail to reject the null hypothesis. The first period, 1928–39, is marked by the intersection of

the time series (due to the steady upward trend of the 20CR-based curve). The second period, 1986–2004, is the period when the time series almost completely agree with each other.

3. Changes in the station density and storminess

Inhomogeneities caused by changes in the station density and quality of observations represent a likely reason for explaining the described discrepancies. The 20CR ensemble spread (regarded for the surface pressure fields) represents the uncertainty in pressure measurements. It further reflects, to a certain degree, the number (or lack) of assimilated pressure observations over land and sea.

From 1871 onward we calculated the yearly mean of the area average of the ensemble standard deviation of the surface pressure over all grid points in the examined area, which roughly spans from 51.9° to 71°N, 22.7°W to 14.5°E (Fig. 3a). Further, to illustrate the number of assimilated stations, we analyzed the metadata provided by Compo et al. (2011) (available at ftp://ftp.ncdc.noaa.gov/pub/data/ispd/v2.2.4/). In an ad hoc manner we counted the number of assimilated land stations in 20CR over the examined area from these metadata (Fig. 3b), which we use as a best guess for the real number of assimilated stations.

The standard deviation steeply decreases until 1880. Afterward, which marks the relevant period in our analyses, the standard deviation slowly decreases until 1938. During the World War II era, we see a steep increase and decrease thereafter (around 1940). After the 1950s the time series decreases further slowly and remains almost unchanged after 1965.

The number of assimilated stations slowly increases until 1927. Afterward, during the World War II era, we see a steep increase followed by a decrease. The time series increases again slowly until the 1960s when it soars to a higher level. In the beginning of the 1970s there is a sudden decline, which is followed again by an increase. It may be possible that there are some gaps in the metadata in this instance. After the mid-1970s, the numbers of assimilated stations are on a high level and increase even further.

Our 20CR-based and observation-based storminess time series agree in their phase characteristics, as written above, from the 1940s onward. From the 1960s onward, even the differences between the time series become smaller and almost vanish. These agreements coincide with the strong reduction of uncertainty in the 20CR ensemble (as in Fig. 3a), also due to the strong increase in the number of assimilated station readings to a high level (Fig. 3b and Compo et al. 2011).

Further, the upward trend in 20CR storminess until the 1950s occurs at the same time when the standard
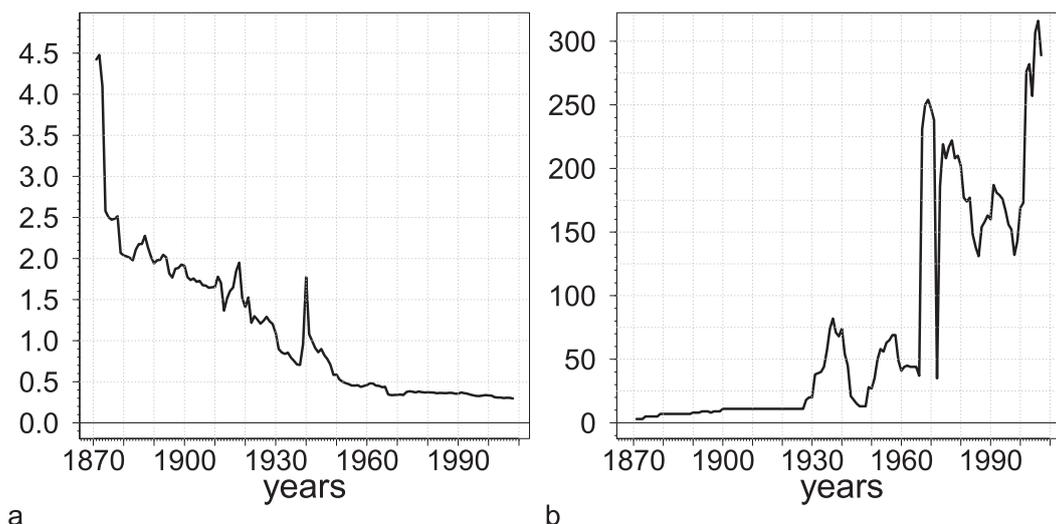
FIG. 3. (a) Yearly-mean values of the area-averaged 20CR ensemble standard deviation of the surface pressure (hPa): all grid points from 51.9° to 71°N, 22.7°W to 14.5°E have been averaged. (b) The number of assimilated stations in 20CR from 51.9° to 71°N, 22.7°W to 14.5°E determined from metadata provided by Compo et al. (2011).

deviation of the 20CR ensemble is steadily decreasing and when the number of assimilated stations is steadily increasing. Over the period 1881–1950, for instance, the low-pass filtered ensemble mean of extreme geostrophic wind speed percentiles and the ensemble standard deviation share a correlation of about −0.60 (about 36% explained variability) due to the opposite trends of the geostrophic wind speed percentiles and the standard deviation.

4. Discussion and conclusions

We have compared long-term time series of storminess over Northern Europe and the northeast Atlantic derived from observations and 20CR. We have assessed the temporal evolution of storminess through a well-established proxy of storm activity. This proxy is based on upper percentiles of geostrophic wind speeds, which we have derived from surface pressure triangles. While both time series share a common behavior roughly during the second part of the twentieth century, they are inconsistent during the earlier years. While the storm index derived from observations shows pronounced decadal variability but no clear long-term trend, the storm index derived from 20CR suggests a more steadily increasing upward trend throughout the twentieth century.

We argue that the long-term behavior of storm activity in 20CR is implausible because of several reasons. A number of studies that examined storminess in that area and used different sources of information support our results, which are based on observed pressure data. Von Storch and Reichardt (1997) and Weisse and von Storch (2009) analyzed extreme sea levels derived from

tide gauge data in the German Bight in terms of storminess. When changes in the mean sea level were taken into account, this proxy showed pronounced decadal variability with a maximum occurring around 1995, but no clear long-term trend over the last century. Woodworth and Blackman (2002) and Menéndez and Woodworth (2010) examined a quasi-global tide gauge dataset and used similar methods. They were similarly unable to derive significant long-term trends in storm-induced water level variations along European coasts. Further, Bärring and von Storch (2004), who used several proxies based on homogenized air pressure readings from individual stations, described pronounced variability but also found no evident long-term trend.

These results suggest that the long-term trend identified from analyzing 20CR needs to be carefully regarded and probably reflects inhomogeneities in the reanalysis itself, most likely as a consequence of a changing station density. A similar argument is stated in Compo et al. (2011), who noted that storm tracks estimated from the ensemble mean of 20CR appear to be noticeably weaker for the earlier period 1887–1947 compared to the more recent period 1948–2008. They emphasize, that "such a result should not be taken as indicative of an actual climate change. Rather, as the observational density gets lower, less synoptic variability is present in the ensemble mean analyses as fewer observations are available."

Our results from analyzing a storm proxy based on large-scale atmospheric pressure data point to inconsistencies in the long-term trends and variability of storminess derived from observations and 20CR. The inconsistencies are largest during the first half of 20CR,

when fewer stations are assimilated and storm activity is surprisingly low. The inconsistencies are already large over a supposedly well-monitored region. Our findings suggest that similar problems may arise, in particular over more data-sparse regions. While changes in the number of assimilated stations appear to be the most likely reason to explain the discrepancies, a 20CR dataset whose station density remains constant over time is required to fully address this problem (e.g., Thorne and Vose 2010). Unfortunately such a dataset is not available so far.

REFERENCES

Alexandersson, H., T. Schmith, K. Iden, and H. Tuomenvirta, 1998: Long-term variations of the storm climate over NW Europe. *Global Atmos. Ocean Syst.,* **6,** 97–120.

——, H. Tuomenvirta, T. Schmith, and K. Iden, 2000: Trends of storms in NW Europe derived from an updated pressure data set. *Climate Res.,* **14,** 71–73.

Bärring, L., and H. von Storch, 2004: Scandinavian storminess since about 1800. *Geophys. Res. Lett.,* **31,** L20202, doi:10.1029/2004GL020441.

Bengtsson, L., S. Hagemann, and K. I. Hodges, 2004: Can climate trends be calculated from reanalysis data? *J. Geophys. Res.,* **109,** D11111, doi:10.1029/2004JD004536.

Bromwich, D. H., R. L. Fogt, K. I. Hodges, and J. E. Walsh, 2007: A tropospheric assessment of the ERA-40, NCEP, and JRA-25 global reanalyses in the polar regions. *J. Geophys. Res.,* **112,** D10111, doi:10.1029/2006JD007859.

Brönnimann, S., O. Martius, H. von Waldow, C. Welker, J. Luterbacher, G. P. Compo, P. D. Sardeshmukh, and T. Usbeck, 2012: Extreme winds at northern mid-latitudes since 1871. *Meteor. Z.,* **21,** 13–27.

Cappelen, J., E. Laursen, and C. Kern-Hansen, 2010: DMI daily climate data collection 1873-2010, Denmark, the Faroe Islands and Greenland. Danish Meteorological Institute Tech. Rep. 11-06, 41 pp. [Available online at http://www.dmi.dk/dmi/tr11-06.pdf.]

Compo, G. P., and Coauthors, 2011: The Twentieth Century Reanalysis project. *Quart. J. Roy. Meteor. Soc.,* **137,** 1–28.

Donat, M. G., D. Renggli, S. Wild, L. V. Alexander, G. C. Leckebusch, and U. Ulbrich, 2011: Reanalysis suggests long-term upward trends in European storminess since 1871. *Geophys. Res. Lett.,* **38,** L14703, doi:10.1029/2011GL047995.

Ferguson, C. R., and G. Villarini, 2012: Detecting inhomogeneities in the Twentieth Century Reanalysis over the central United States. *J. Geophys. Res.,* **117,** D05123, doi:10.1029/2011JD016988.

Glickman, T., Ed., 2000: *Glossary of Meteorology.* 2nd ed. Amer. Meteor. Soc., 855 pp.

Kalnay, E., and Coauthors, 1996: The NCEP/NCAR 40-Year Reanalysis Project. *Bull. Amer. Meteor. Soc.,* **77,** 437–471.

Kistler, R., and Coauthors, 2001: The NCEP–NCAR 50-Year Reanalysis: Monthly means CD-ROM and documentation. *Bull. Amer. Meteor. Soc.,* **82,** 247–267.

Krueger, O., and H. von Storch, 2011: Evaluation of an air pressure–based proxy for storm activity. *J. Climate,* **24,** 2612–2619.

Lindenberg, J., H. Mengelkamp, and G. Rosenhagen, 2012: Representativity of near surface wind measurements from coastal stations at the German Bight. *Meteor. Z.,* **21,** 99–106.

Madden, R. A., and R. H. Jones, 2001: A quantitative estimate of the effect of aliasing in climatological time series. *J. Climate,* **14,** 3987–3993.

Matulla, C., W. Schöner, H. Alexandersson, H. von Storch, and X. Wang, 2008: European storminess: Late nineteenth century to present. *Climate Dyn.,* **31,** 125–130.

Menéndez, M., and P. Woodworth, 2010: Changes in extreme high water levels based on a quasi-global tide-gauge data set. *J. Geophys. Res.,* **115,** C10011, doi:10.1029/2009JC005997.

Onogi, K., and Coauthors, 2007: The JRA-25 Reanalysis. *J. Meteor. Soc. Japan,* **85,** 369–432.

Schmidt, H., and H. von Storch, 1993: German Bight storms analysed. *Nature,* **365,** 791–793.

Schmith, T., 1995: Occurrence of severe winds in Denmark during the past 100 years. *Proc. Sixth Int. Meeting on Statistical Climatology,* Galway, Ireland, All-Ireland Statistics Committee and Cosponsors, 83–86.

Thorne, P. W., and R. S. Vose, 2010: Reanalyses suitable for characterizing long-term trends. *Bull. Amer. Meteor. Soc.,* **91,** 353–361.

Trenberth, K. E., and Coauthors, 2007: Observations: Surface and atmospheric climate change. *Climate Change 2007: The Physical Science Basis,* S. Solomon et al., Eds., Cambridge University Press, 235–336.

Uppala, S. M., and Coauthors, 2005: The ERA-40 Re-Analysis. *Quart. J. Roy. Meteor. Soc.,* **131,** 2961–3012.

Von Storch, H., and H. Reichardt, 1997: A scenario of storm surge statistics for the German Bight at the expected time of doubled atmospheric carbon dioxide concentration. *J. Climate,* **10,** 2653–2662.

Wan, H., X. L. Wang, and V. R. Swail, 2010: Homogenization and trend analysis of Canadian near-surface wind speeds. *J. Climate,* **23,** 1209–1225.

Wang, X., F. Zwiers, V. Swail, and Y. Feng, 2009: Trends and variability of storminess in the northeast Atlantic region, 1874–2007. *Climate Dyn.,* **33,** 1179–1195.

Weisse, R., and H. von Storch, 2009: *Marine Climate and Climate Change: Storms, Wind Waves and Storm Surges.* Springer Praxis, 219 pp.

Woodworth, P., and D. Blackman, 2002: Changes in extreme high waters at Liverpool since 1768. *Int. J. Climatol.,* **22,** 697–714.

Acknowledgements